ENVIRONMENTAL AND DEMOGRAPHIC DRIVERS OF A RAPIDLY EXPANDING SUB-ARCTIC MOOSE POPULATION

By

Vassily Sebastian Zavoico, B.A.

A Thesis Submitted in Partial Fulfillment of the Requirements

for the Degree of

Master of Science

in

Wildlife Biology & Conservation

University of Alaska Fairbanks

May 2023

APPROVED:

Dr. Shawn Crimmins, Committee Chair
Dr. Joseph Eisaguirre, Committee Member
Dr. Christa Mulder, Committee Member
Dr. Ken Tape, Committee Member
Dr. Todd Brinkman, Program Chair
Wildlife Biology & Conservation Program
Dr. Karsten Hueffer, Interim Dean
College of Natural Sciences & Mathematics
Dr. Richard Collins, Director
Graduate School

Abstract

Anthropogenic forces are dramatically altering the dynamics of many populations and ranges. A thorough understanding of drivers and mechanisms underlying population dynamics is needed to better understand reasons for range shifts and broaden our understanding of how environmental and demographic drivers affect population trajectories. In this thesis, I present two chapters that investigate the population dynamics of a rapidly colonizing moose (*Alces alces*) population in southwest Alaska. In the first chapter, I correlated environmental variables with demographic rates estimated using a multistate model and found that annual patterns of vegetation productivity and winter severity affected calf survival most strongly, followed by twinning rate. In the second chapter, I applied transient life table response experiments (tLTREs) to demographic rates and components of population structure estimated using an integrated population model (IPM). I found that, although calf survival did not have the highest sensitivity out of all other parameters, variation in calf survival contributed the most to variation in population growth rate. Together, these chapters suggest that variation in environmental conditions drove variation in population growth rate via effects on calf survival. Results uphold and add nuance to the demographic buffering hypothesis (DBH), which states that species evolve to buffer highest sensitivity demographic rates against variation that could otherwise decrease individual fitness and population sustainability. My research indicates that an outcome of the DBH is that lower sensitivity vital rates ultimately have a higher actual impact on population growth rate. Additionally, I found that the environmental drivers that currently limit population growth exhibit long-term trends consistent with climate change in ways that are amenable to moose, which suggests climate change facilitated moose colonization of the region. The lack of short-term trends, lower adult survival in the most heavily hunted part of the study area, and the abrupt colonization that aligned with the irruption of a local caribou (*Rangifer tarandus*) herd indicate that human hunting pressure also played an important role in allowing moose to establish themselves at high density. These findings pertaining to drivers and mechanisms

of population dynamics are relevant for conservation and management of large herbivores across the world that might similarly expand into new areas.

Table of Contents

List of Figures

List of Tables

Page

Acknowledgments

I am indebted to a long list of friends, colleagues, mentors, teachers, and family members to whom I attribute my inspiration, motivation, and sense of joy and wonder.

I first want to thank my parents, Martina and Basil and brother, Benny, for their unwavering support from Day 1. Thank you for putting up with my wild ideas, and for being behind my back even when my aspirations take me far away from home. I am grateful to the many educators that have gotten me here, from Ms. Khanna and Ms. Chong in primary school, to Mr. George, Ms. Ward, Ms. Roberts, Dr. Ricketts, and Mr. Sabin who inspired creativity and having fun in learning in high school. Many thanks to Drs. Dave Allen, Helen Young and many others in the Middlebury College Biology Department, as well as Drs. Mads Forchhammer and Nick Tyler in Norway for supporting me through my undergraduate career. Mads, you are missed in this world.

In Fairbanks, big thanks to my advisor, Shawn Crimmins, and my committee for their constructive feedback, helpful discussions, and the right amount of prodding to get me where I am on this circuitous and difficult journey. Thanks especially to Joe Eisaguirre for his patient and expert guidance with the statistics behind this project. I carry so much gratitude for those in the Ecology Reading Group for grounding discussions, jovial banter (most important), and inspiration towards critical thinking, including but not limited to Greg, Shawn, Abigail, Sarah, Derek, Luke, Laura, Brendan, Matt, Jess, Cody, and Scott. Outside of UAF, I am indebted to incredible friends and adopted family that have kept me afloat and steered in the right direction through the Masters and pandemic, including but not limited to those in the reading group, Harper, Tricia, the Hewitt family, Jake, Hannah, Taylor, Cherissa, Arleigh, Luka, Brie, and Stefan. Thank you all for the food, skiing, biking, camping, cabin trips, board games, and co-journeying through humanhood.

Many thanks to everyone in Dillingham who made that small town a home away from home for two summers. I am grateful for everyone in Togiak NWR for housing me and providing invaluable experiences, including Andy, Kara, Pat, Stan, Jack, Derek, Terry and Kenton. Cheers to everyone else in Dillingham who made living there so special, especially Jannelle, Brian and the rest of the Venua family, Teresa, Ali, Truett, Mariah, and Deven and the rest of the Lisac family. Thank you all for the home brews, the music nights, garden time, boating, the fishing, the fishing, and the fishing.

I acknowledge that I lived and worked on Lower Tanana Dené and Yup'ik people's land for this work, and am grateful for their enduring stewardship of these most beautiful and sacred lands that I continue to gain so much from. Maasee', Quyana.

Chapter 1: General Introduction

While life histories and population dynamics of large herbivores have been studied extensively (Gaillard et al., 2000; Gaillard and Yoccoz, 2003), it remains unclear how patterns of survival and reproduction actually affect population growth. This is because most studies rely on methods that estimate environmental and demographic impacts on asymptotic growth rate (Caswell, 1989, 2000; Wisdom et al., 2000), which only encapsulates an overall trend of the population. A more powerful method, transient life table response experiments (tLTRE), decomposes overall trends into growth rate in between relevant time steps, or realized growth rate (Koons et al., 2016, 2017). Focusing analysis on these observed, rather than potential, growth rates allows for more detailed knowledge of how environmentally induced fluctuations in demographic rates drive variation in population growth rates (Tuljapurkar, 2010). Understanding how the environment has driven population dynamics is more important than ever, as climate change alters the Earth's ecosystems.

Retrospective analysis of environmental factors — which can include weather, food availability, and disease — on population dynamics can disentangle the complex innerworkings of populations. This is because environmental impacts can depend on species (Berteaux and Stenseth, 2006), population structure (e.g Maldonado-Chaparro et al., 2018), interspecific competition (e.g Keech et al., 2011), and intraspecific competition (e.g Koons et al., 2015), to name a few. It is therefore important to account for as much as possible given prior knowledge of the species, population, and surrounding ecosystem. Additionally, because population dynamics are often tied to movement of species and populations (Sexton et al., 2009), understanding what environmental factors are limiting population growth can illuminate reasons for events like colonization. This is particularly pertinent as many species ranges are transforming as the climate warms (Chen et al., 2011).

Moose (*Alces alces*) are an excellent study species that can be used to deepen our knowledge of more general relationships between the environment, demographics, and population dynamics. The species has been studied intensively, as it is culturally, economically, and socially important to societies across the northern hemisphere (Franzmann and Schwartz, 1998; Rosa et al., 2020). There are thus numerous long-term studies to facilitate comparison to (see Franzmann and Schwartz, 1998; Gaillard et al., 2000; Boertje et al., 2007). Moose are also physiologically and behaviorally plastic (Wattles et al., 2018) and can disperse long distances (Ballard et al., 1991), making them highly adaptable to changing environmental conditions. Moose are relative newcomers to North America, having only arrived 15,000 years ago (Hundertmark and Bowyer, 2004; Meiri et al., 2020), and are expanding the extents of both southern (Wolfe et al., 2010; Wattles et al., 2018) and northern (Chubbs and Schaefer, 1997; Tape et al., 2016; Rosa et al., 2020) ranges. The reasons for these expansions have not been empirically tested, though hypotheses converge on a mixture of climate change increasing food availability (Tape et al., 2016; Rosa et al., 2020) and direct human influences improving survival (Tape et al., 2016; Wattles et al., 2018).

The moose population in Togiak National Wildlife Refuge (TNWR) in southwest Alaska, USA, is a population that has recently expanded and has also been monitored long-term. Moose existed in low densities from at least the mid-19th century (Abercrombie et al., 1900), but expanded from approximately a dozen individuals in the 1980s to over 3000 in 2017 (Aderman, 2014; Aderman et al., 2019). The rapid increase occurred concomitantly with a statewide 2.1°C increase in winter temperatures (Walsh and Brettschneider, 2019) that has resulted in a higher frequency of mild winters (Callaghan et al., 2011; Lader et al., 2020), and a 1.3°C increase in summer temperatures (Walsh and Brettschneider, 2019) that may have caused an increase in deciduous shrub cover (Swanson, 2015; Macander et al., 2022) in suitable moose habitat. Humans have inhabited TNWR since time immemorial, and also likely played a role in this increase; the initial wave of moose population growth occurred

during the Mulchatna caribou herd irruption in the 1980s and 1990s (Valkenburg et al., 2003) that likely diverted hunting pressure from moose to preferred caribou (Aderman, 2014).

In this thesis, I investigate environmental and demographic drivers of moose population dynamics in TNWR to both (1) Answer the question of why the abundance of moose in TNWR increased so rapidly, and (2) Broaden our understanding of how environmental variation affects population growth rate through impacts on demographic rates. In the first chapter, I correlated environmental conditions with demographic rates estimated from a long-term radio telemetry dataset. I accounted for important demographic and anthropogenic conditions, including age, lifetime individual heterogeneity, and hunting management area inhabited by each moose. In the second chapter, I decomposed variance into annual demographic rates and components of population structure to calculate the contributions to variance of population growth rates. The models in these chapters are novel to moose and most ungulates, and build on to each other: the multistate model that estimates demographic rates in chapter 1 is integrated with a count state-space model to form an integrated population model (IPM) (Schaub and Kery, 2021) that estimates abundance and demographic rates.

1.1 References

Abercrombie, W. R., E. F. Glenn, O. O. Howard, I. Petroff, P. H. Ray, W. P. Richardson, and E. H. Wells (1900). *Compilation of Narratives of Explorations in Alaska.* Number 1023. US Government Printing Office.

Aderman, A. (2014). Monitoring moose demographics at Togiak National Wildlife Refuge, southwestern Alaska, 1998-2013. *Togiak National Wildlife Refuge, Dillingham, Alaska.*, 1–25.

Aderman, A., N. Barten, and M. Higham (2019). Estimation of moose abundance using the geospatial population estimator combined with a sightability model on Togiak NWR; final project report. *Western Alaska Landscape Conservation Cooperative Project*, 1–16.

Ballard, W. B., J. S. Whitman, and D. J. Reed (1991). Population dynamics of moose in south-central Alaska. *Wildlife Monographs*, 3–49.

Berteaux, D. and N. C. Stenseth (2006). Measuring, understanding and projecting the effects of large-scale climatic variability on mammals. *Climate Research 32*(2), 95–97.

Boertje, R. D., K. A. Kellie, C. T. Seaton, M. A. Keech, D. D. Young, B. W. Dale, L. G. Adams, and A. R. Aderman (2007). Ranking Alaska moose nutrition: Signals to begin liberal antlerless harvests. *Journal of Wildlife Management 71*, 1494–1506.

Callaghan, T. V., M. Johansson, R. D. Brown, P. Y. Groisman, N. Labba, V. Radionov, R. G. Barry, O. N. Bulygina, R. L. H. Essery, and D. M. Frolov (2011). The changing face of arctic snow cover: A synthesis of observed and projected changes. *Ambio 40*, 17–31.

Caswell, H. (1989). Analysis of life table response experiments I. Decomposition of effects on population growth rate. *Ecological Modelling 46*, 221–237.

Caswell, H. (2000). *Matrix population models*, Volume 1. Sinauer Sunderland.

Chen, I. C., J. K. Hill, R. Ohlemüller, D. B. Roy, and C. D. Thomas (2011). Rapid range shifts of species associated with high levels of climate warming. *Science 333*, 1024–1026.

Chubbs, T. E. and J. A. Schaefer (1997). Population growth of moose, *Alces alces*, in Labrador. *Canadian Field Naturalist 111*, 238–242.

Franzmann, A. W. and C. C. Schwartz (1998). *Ecology and Management of the North American Moose* (1 ed.). Wildlife Management Institute.

Gaillard, J.-M., M. Festa-Bianchet, N. G. Yoccoz, A. Loison, and C. Toigo (2000). Temporal variation in fitness components and population dynamics of large herbivores. *Annual Review of Ecology and Systematics 31*, 367–393.

Gaillard, J.-M. and N. G. Yoccoz (2003). Temporal variation in survival of mammals: a case of environmental canalization? *Ecology 84*, 3294–3306.

Hundertmark, K. J. and R. T. Bowyer (2004). Genetics, evolution, and phylogeography of moose. *Alces: A Journal Devoted to the Biology and Management of Moose 40*, 103–122.

Keech, M. A., M. S. Lindberg, R. D. Boertje, P. Valkenburg, B. D. Taras, T. A. Boudreau, and K. B. Beckmen (2011). Effects of predator treatments, individual traits, and environment on moose survival in Alaska. *Journal of Wildlife Management 75*, 1361–1380.

Koons, D. N., T. W. Arnold, and M. Schaub (2017). Understanding the demographic drivers of realized population growth rates. *Ecological Applications 27*(7), 2102–2115.

Koons, D. N., F. Colchero, K. Hersey, and O. Gimenez (2015). Disentangling the effects of climate, density dependence, and harvest on an iconic large herbivore's population dynamics. *Ecological Applications 25*(4), 956–967.

Koons, D. N., D. T. Iles, M. Schaub, and H. Caswell (2016). A life-history perspective on the demographic drivers of structured population dynamics in changing environments. *Ecology Letters 19*, 1023–1031.

Lader, R., J. E. Walsh, U. S. Bhatt, and P. A. Bieniek (2020). Anticipated changes to the snow season in Alaska: Elevation dependency, timing and extremes. *International Journal of Climatology 40*, 169–187.

Macander, M. J., P. R. Nelson, T. Nawrocki, G. V. Frost, K. Orndahl, E. C. Palm, A. F. Wells, and S. J. Goetz (2022). Time-series maps reveal widespread change in plant functional type cover across arctic and boreal Alaska and Yukon. *Environmental Research Letters 17*(5), 054042.

Maldonado-Chaparro, A. A., D. T. Blumstein, K. B. Armitage, and D. Z. Childs (2018). Transient ltre analysis reveals the demographic and trait-mediated processes that buffer population growth. *Ecology letters 21*(11), 1693–1703.

Meiri, M., A. Lister, P. Kosintsev, G. Zazula, and I. Barnes (2020). Population dynamics and range shifts of moose (*Alces alces*) during the Late Quaternary. *Journal of Biogeography 47*, 2223–2234.

Rosa, K., C. Dale, J. Purcell, M. Wood, and J. Snook (2020). Inuit knowledge and values of moose in Nunatsiavut Torngat Wildlife and Plants Co-Management Board. *Torngat Wildlife, Plants and Fisheries Secretariat Series*, 1–70.

Schaub, M. and M. Kery (2021). *Integrated population models: theory and ecological applications with R and JAGS*. Academic Press.

Sexton, J. P., P. J. McIntyre, A. L. Angert, and K. J. Rice (2009). Evolution and ecology of species range limits. *Annual Review of Ecology, Evolution and Systematics 40*(1), 415–436.

Swanson, D. K. (2015). Environmental limits of tall shrubs in Alaska's Arctic national parks. *PLoS ONE 10*.

Tape, K. D., D. D. Gustine, R. W. Ruess, L. G. Adams, and J. A. Clark (2016). Range expansion of moose in arctic Alaska linked to warming and increased shrub habitat. *PLoS ONE 11*.

Tuljapurkar, S. (2010). Environmental variance, population growth and evolution. *Journal of Animal Ecology 79*(1), 1–3.

Valkenburg, P., R. A. Sellers, R. C. Squibb, J. D. Woolington, A. R. Aderman, and B. W. Dale (2003). Population dynamics of caribou herds in southwestern Alaska. *Rangifer 23*(5), 131–142.

Walsh, J. E. and B. Brettschneider (2019). Attribution of recent warming in Alaska. *Polar Science 21*, 101–109.

Wattles, D. W., K. A. Zeller, and S. DeStefano (2018). Range expansion in unfavorable environments through behavioral responses to microclimatic conditions: Moose (*Alces americanus*) as the model. *Mammalian Biology 93*, 189–197.

Wisdom, M. J., L. S. Mills, and D. F. Doak (2000). Life stage simulation analysis: estimating vital-rate effects on population growth for conservation. *Ecology 81*(3), 628–641.

Wolfe, M. L., K. R. Hersey, and D. C. Stoner (2010). A history of moose management in Utah. *Alces 46*, 37–52.

Chapter 2: Environmental and anthropogenic drivers of a rapidly expanding sub-arctic ungulate population[1]

2.1 Abstract

Species are shifting distributions in response to climate change worldwide, with range expansions already apparent in high-latitude biomes. Reasons for distribution shifts can vary by species and region, and it is important to understand these drivers when a species is of ecological and economic importance. We investigated environmental drivers of a moose (*Alces alces*) population that increased at least 400-fold from 1991–2017, in Togiak National Wildlife Refuge in southwest Alaska, USA. This population and range expansion occurred simultaneously with rising temperatures, shrubification, increasingly inconsistent winter snowpack, and varying management strategies. We tested the hypothesis that climate change and management facilitated this population expansion by studying moose population dynamics from 1998–2020 to better understand the reasons for the species' range expansion. We used a multistate model to estimate annual vital rates from monthly telemetry observations, and modeled vital rates as functions of covariates to test relationships between each vital rate, components of climate change in the region, and Game Management Units. Probabilities of calf survival and twinning increased in or after years of higher vegetation productivity (NDVI), and lower winter severity (WSI). Parturition probability correlated weakly and negatively with WSI, and cow survival correlated weakly and positively with NDVI. Additionally, differences in cow survival between management units indicated that human hunting pressure influenced population dynamics. While we did find that environmental conditions explained variation in vital rates, the moose population grew while neither NDVI nor WSI showed trends over the study time period. NDVI and WSI did correlate with long-term temperature increase, however, which indicates that, at least historically, elements of climate

[1]Zavoico, VS, JM Eisaguirre, SM Crimmins, AA Aderman, CPH Mulder, GG Frye, MA Cobb, MS Lindberg. 2023. Environmental and anthropogenic drivers of a rapidly expanding sub-arctic ungulate population. Prepared for submission: Ecology and Evolution.

change and hunting pressure facilitated population expansion of this sub-arctic ungulate, and will continue to do so. Our study uncovers possible reasons for ungulate colonization of high-latitude systems, but more work is necessary to account for density-dependence and understand what impact calf survival and twinning have on population growth rate.

2.2 Introduction

Species worldwide are shifting their distributions in response to climate change (Chen et al., 2011; Bellard et al., 2012). The drivers of these range shifts are many and diverse, as environmental changes are variable, and species and populations may respond differently to the same stressors. Understanding the reasons for these distribution shifts can help predict future community composition, especially in the Arctic, where mean surface temperatures are increasing at three times that of the global average (Secretariat, 2021). The response of herbivores to changing environmental conditions is important to understand because they can have a large impact on ecosystem change, as they can affect plant species composition and growth (Kielland and Bryant, 1998; Christie et al., 2015) and plant resilience to climate change (Vuorinen et al., 2020). Some herbivores have substantially expanded their ranges in regions of the Arctic and sub-Arctic in recent decades (Tape et al., 2016, 2022) for reasons that have thus far not been quantitatively examined. By untangling the drivers of herbivore population changes along the northern edges of their ranges, we can better predict how species ranges, and thus what community composition, may look like in the future. Predicting population trajectories is particularly important for arctic and sub-arctic large herbivores, which have cultural and economic value as subsistence and hunting resources.

One potential factor aiding large herbivore range expansion is increasing vegetation availability. The Arctic is, overall, "greening", a likely outcome of increased plant biomass and a proliferation of tall shrub species (Epstein et al., 2013). This last phenomenon has been coined "shrubification" and describes both the increasing growth in previously occupied areas

and the rapid colonization of previously unoccupied areas (Tape et al., 2006; Myers-Smith et al., 2011; Epstein et al., 2013). For example, up to a third of tundra vegetation has transitioned to tall shrub habitat over 60 years in northwest Alaska (Terskaia et al., 2020) and shrub-dominated vegetation area has doubled over 50 years in northern Alaska (Sturm et al., 2001). Shrubification will likely benefit those large herbivores that eat tall shrubs (Tape et al., 2016, 2018) by increasing forage productivity (Zhou et al., 2017) and habitat connectivity (Zhou et al., 2020). Rising temperatures as a component of climate change is a key driver for shrubification across the Arctic, along with soil disturbance and herbivory (Myers-Smith et al., 2011). Thus, climate change could indirectly promote range expansion of large herbivores by increasing forage availability.

Another potential factor aiding large herbivore range expansion is changing winter conditions. Winters in the Arctic and sub-Arctic are becoming less severe, with higher average temperatures (Walsh and Brettschneider, 2019) and more frequent rain events (Lader et al., 2020). Coastal areas are particularly affected, where decreasing sea ice extent compounds winter warming and shifts continental climates to warmer, wetter maritime climates (Callaghan et al., 2011; Lader et al., 2020). Unlike shrubification, where advantages for herbivores are clearer, it is unclear how changes in winter conditions will affect herbivores. While factors like later fall snow onset can increase individual body weight and thus population growth rate (Loe et al., 2021), more variable snow depth and density can increase physiological exertion (Sweanor and Sandegren, 1989; Ballard et al., 1991; Ball et al., 2001; Keech et al., 2011). More specifically, exertion from foraging and movement in deep snow increases predation risk (Robinson and Merrill, 2012) and reduces body condition (Keech et al., 2011; Cosgrove et al., 2021), both of which decrease winter survival. Deep snow can also decrease reproduction rates, where lower body condition from high exertion can lead to failed pregnancies (Testa and Adams, 1998). Therefore, lower winter severity as a result of climate change might facilitate range and population expansion for large herbivores by

reducing physiological limitations in the winter.

Large herbivores not only inhabit complex ecological systems, but are also often interwoven into human systems. A potential cause for large herbivore colonization of the Arctic is release from human hunting pressure that either prevented populations from inhabiting the edges of their ranges, or maintained populations at low densities (Aderman, 2014; Tape et al., 2016, 2018). In southwest Alaska, competing hunting pressure with a local irrupting caribou (*Rangifer tarandus*) population and a moose (*Alces alces*) hunting moratorium in a Game Management Unit (GMU) might have allowed moose to rapidly colonize an area where they had previously existed in low densities (Aderman, 2014).

Moose likely benefit from the changing winter, vegetation, and hunting dynamics of the Arctic. They exhibit physiological and behavioral plasticity at the edges of distribution extremes (Wattles et al., 2018) and can disperse long distances (Ballard et al., 1991), making them adaptable to changing environmental conditions. For example, moose populations along their northernmost ranges in North America have expanded into new territories in the Canadian provinces of Labrador and Quebec (Chubbs and Schaefer, 1997; Rosa et al., 2020) and across the North Slope of the US state of Alaska (Tape et al., 2016). In both cases, increases in moose abundance occurred concurrently with shrubification (Tape et al., 2016; Rosa et al., 2020), and on the North Slope, abundance increased alongside decreasing hunting pressure (Tape et al., 2016). No study has yet, however, directly linked environmental and anthropogenic changes to increased population productivity that drove these kinds of colonization events.

An investigation of dynamics of a colonizing moose population must consider intrinsic demographic variation inherent in all mammal populations, and the ecology specific to a colonizing one. Age senescence is intrinsic to any placental mammal population, where female

fecundity decreases later in life (Loison et al., 1999; Ericsson et al., 2001). Thus, average age of the population can change population dynamics and must be considered. Not all females are equally fecund, however, and the effect of individual phenotypic and genotypic heterogeneity can affect population dynamics as well (Chambert et al., 2013; Badger et al., 2020). Finally, colonizing populations are potentially subject to different stressors than more established populations; for one, they can be more subject to bottom-up, rather than top-down effects as predators may not cue into new food sources immediately (such as lack of brown bear (*Ursus arctos*) predation in Kaji et al. (2004)). Colonizing populations are also subject to rapidly increasing levels of density-dependence as populations approach carrying capacity from near-zero density (Kaeuffer et al., 2010). Therefore, any investigation of biotic and abiotic effects on a colonizing population should at least take into account age senescence, individual heterogeneity, predation dynamics, and density dependence.

We investigated effects of changing climate and hunting pressures on population dynamics in a colonizing moose population of the sub-Arctic. Moose in Togiak National Wildlife Refuge (TNWR) in southwest Alaska existed at low densities (Abercrombie et al., 1900) until the 1980s (Aderman, 2014). From 1991 to 2017, the moose population increased at least 400-fold (Aderman, 2014; Aderman et al., 2019), and colonized far western reaches of TNWR, along and beyond the longitudinal tree- and shrub-line (Viereck, 1979). The population increase occurred concomitantly with a statewide 2.1°C increase in winter temperatures (Walsh and Brettschneider, 2019) that has resulted in a higher frequency of mild winters (Callaghan et al., 2011; Lader et al., 2020), a 1.3°C increase in summer temperatures (Walsh and Brettschneider, 2019) that may have caused an increase in deciduous shrub cover (Macander et al., 2022), and hunting pressure change (Aderman, 2014). We thus tested competing hypotheses that high population productivity is facilitated either by climate change or altering hunting pressure, or both, while accounting for intrinsic demographic variability. We represented climate change using metrics of winter severity and vegetation productivity,

hunting pressure using inhabited GMUs, and demographic variability using age and individual heterogeneity. We tested hypotheses by correlating covariates to annual demographic parameter estimates in a Bayesian hierarchical multistate model that used 24 years of radio telemetry data collected for 106 individual moose. We considered our climate change hypothesis supported if moose demographic rates were 1) positively associated with vegetation productivity and 2) negatively associated with winter severity. We considered our hunting hypothesis supported if cow survival was lowest in GMUs without hunting moratoriums, and highest in GMUs with hunting moratoriums.

2.3 Methods

2.3.1 Study Area

We analyzed radio telemetry and environmental data collected in and around Togiak National Wildlife Refuge (TNWR) in southwest Alaska, USA. The study area comprises 21,063 km^2 and includes GMUs defined by Alaska Department of Fish & Game, each with differing hunting management histories. Portions of GMUs 17A, 17C, 17B and 18 are located in the study area, and we divided GMU 18 in three according to drainages: 18-Kanektok-Arolik (18KA), 18-Goodnews (18G), and 18-Eek (18E) (Figure 2.1) to accommodate a moose hunting moratorium that took effect in 18G from 2003–2006 to increase cow survival, but didn't take effect in 18KA. As 18E and 17B represent a small area of TNWR, and were not subject to hunting moratoriums, we added them to 18KA and 17C, respectively. TNWR is in a transitional climate zone, with both maritime and continental influences on weather patterns. Maritime influence generally decreases with distance to open water, but becomes dynamic in winter and spring as sea ice cover changes distance from the coast. Average summer temperature in King Salmon, AK, the closest long-term weather station (Figure 2.1) is 12.8°C (1991–2020), and average winter temperature is -7°C (Alaska Climate Research Center, 2022b). Annual average precipitation is 54.5cm (1991–2020) (Alaska Climate Research Center, 2022a). TNWR is typically colder, receives more snow, and has a more

durable snowpack than King Salmon (Aderman, unpublished data).

Vegetation in TNWR transitions from alpine tundra in central mountains to upland shrubs on lower slopes, to lowland and coastal tundra communities at sea level. Numerous lakes and rivers support extensive riparian communities that host productive deciduous shrubs and trees, and far eastern valleys include mixed boreal forest. Generally, vegetation productivity and biomass decrease from east to west (Viereck, 1979). Tundra and low or dwarf shrub communities dominate the cover of TNWR (50%), followed by tall shrubs (20%), barren ground (16%), wetland (12%), and forest (2%) (Collins, 2003). Primary tall and dwarf shrub species are alder (*Alnus spp.*), willow (*Salix spp.*), and dwarf birch (*Betula spp.*), and primary forest species are white spruce (*Picea glauca*) and Alaska birch (*Betula neoalaskana*). Caribou from the Mulchatna and Nushagak Pensinsula herds share similar territories as well as human and natural hunting pressure with moose (Valkenburg et al., 2003). Both ungulates are preyed on by wolves (*Canis lupus*), coyotes (*Canis latrans*), wolverines (*Gulo gulo*) and brown bears, though predator abundance is unknown and predation is thought to be low (Aderman, 2014).

2.3.2 Telemetry Data

From 1998–2020, TNWR regularly fitted female adult, yearling, and calf moose with VHF radio collars (Telonics Inc, Mesa, Arizona, USA) equipped with a motion-sensitive mortality switch. VHF collars were replaced when moose lived long enough for collar batteries to die, and new individuals were collared every ∼5 years to maintain sufficient sample size and a representative age distribution. Observers used fixed-wing aircraft to locate and determine calf association for each cow, and attempted to locate each individual once per month, but concentrated efforts during birthing months (May-June), the fall (November) and late winter (February-March). Due to various constraints, many individuals were not observed monthly. When observers heard a mortality signal, they located the individual as soon as possible to

confirm mortality. We calculated day of death as the median date in between the last live, and the first dead observation. Dates were recorded as day-of-year with respect to the first day of parturition (May 14).

2.3.3 Covariates

We tested hypotheses regarding climate effects on moose demographics using metrics of vegetation productivity and winter severity calculated from remotely sensed and weather data. For remotely sensed data, we collected TNWR-wide Normalized Difference Vegetation Index (NDVI), a common proxy for vegetation productivity, and Normalized Difference Snow Index (NDSI), which measures percent snow cover. We did this using NASA's Moderate Resolution Imaging Spectroradiometer (MODIS) satellite imagery via Google Earth Engine (Gorelick et al., 2017) for summer (May-mid-September) and winter (November-April), respectively. MODIS satellite sensors have produced global 16-day composite images at 250 m resolution from 2000 to the present year, creating consistent spatial and temporal profiles of the Earth's surface. We quantified annual summer vegetative productivity using Total Integrated NDVI (TIN, but hereafter referred to as NDVI for simplicity), (Potter and Alexander, 2020; Frost et al., 2021) by summing pixels from each composite image into one image, then averaging all pixels within the TNWR boundary for each year. To quantify winter severity, we first used the same method as TIN to produce an average winter NDSI value. We then multiplied the scaled and centered NDSI, absolute value of mean winter temperature (°C) (all years of which were < 0°C, except 2015–2016, which averaged 0.41°C) and total snow accumulation (cm) from King Salmon to produce a Winter Severity Index (WSI). We calculated annual NDVI estimates from 2000–2020, and WSI values from 2001–2019.

As we only had 19–20 years of WSI and NDVI, we needed to ensure they were representative of longer-scale climate change; simple linear correlations of measures over such a short time period might be subject to nonlinear oscillations. We examined how well NDVI and

WSI represented climatic changes by correlating each measure using simple linear regression with year, and the Pacific Decadal Oscillation (PDO) (NOAA, 2022). We included the analysis with PDO because similar oscillations drive environmental processes that affect ungulates elsewhere (Post and Forchhammer, 2002), and because a known PDO phase shift at the end of the 20th century (Kosaka and Xie, 2013) could introduce bias to a linear regression. To further investigate whether NDVI and WSI represent climate change, we correlated King Salmon, AK July and aggregated winter temperatures with the time period we had data for (1970–2020), then correlated NDVI and WSI to King Salmon July and winter temperatures. We assessed correlations using an $\alpha = 0.05$ threshold.

To account for age senescence in the population (Loison et al., 1999), we calculated individuals' ages for every time step. We assumed an age of 0 or 1 when a calf or yearling was collared, and estimated age of adults based on tooth wear. From the age-at-collaring estimate, we then calculated age for all following time steps. Age estimates based on tooth wear can be inaccurate (Hewison et al., 1999), however, so we analyzed all adult ages for all timesteps for outliers, but did not detect any.

To account for different demographic rates according to hunting regulations by GMU, we determined the GMU each moose inhabited over its lifetime. We intersected a 95% Minimum Convex Polygon (MCP) for each individual from lifetime telemetry observations with GMU polygons. We then categorized a moose's home range by GMU if 75% of the MCP overlapped with a GMU. Any moose that overlapped with multiple GMUs was considered to be in "Neither" GMU. Ultimately, 71 moose resided in GMU 17A, 4 in 17C, 15 in 18G, 4 in 18KA, and 12 in neither GMU.

Finally, to assist with model convergence and interpretation, we scaled and centered all continuous covariates to mean = 0 and SD = 1. We set years without covariate values

to 0 (1998–1999 for NDVI, and 1998–2001 & 2020 for WSI). To assess multicollinearity, we calculated Pearson correlation coefficients (ρ) between all variables. No covariate correlations exceeded our ρ =0.6 threshold.

2.3.4 Model Framework

We configured a multistate - a variant of a state-space - model that used monthly observations from 106 cow moose to derive annual estimates of cow survival, calf survival, parturition probability and twinning probability, and to derive a global estimate of calf detection probability. We could only estimate calf detection because observations were only included when collared cows and their potential calves were successfully observed, and not when searched for but not found. Thus cow detection probability was considered perfect, but calf detection was not. We chose a state-space model configured in a Bayesian framework because it accommodated missing observations, and separated process from observational error, which was key in accounting for imperfect calf detection (Kèry and Schaub, 2011; Lebreton et al., 2009). We linked environmental and demographic covariates to annual estimates of survival and reproduction using submodels similar to logistic regressions within our multistate model.

To estimate survival, reproductive, and calf detection parameters, we used two sets of likelihood functions that processed monthly cow observations that we divided into four states: 1) alive without calves, 2) alive with one calf, 3) alive with two calves, and 4) dead. The first set of functions, the state-process functions, described the latent true transitions between states. The second set of functions, the observation-process functions, mapped the true state on the raw data by conditioning the true states on the observations. This set of functions allowed us to account for imperfect detection.

To begin the analysis of any individual, we parameterized likelihoods and matrices that set the state- and observation-processes during the initial capture event, f. Both processes

were set as categorical distributions (Eqs. 2.1 & 2.2) from the matrix $\mathbf{\Omega}$ that determined the state z_{i,f_t} of the ith (i=1,...,I, where I = 106) individual during its capture event, f, at time t (t=1,...,T, where T = 288) (Appendix Table 5.1a),

$$z_{i,f_t} \sim Categorical(\mathbf{\Omega}_{i,f_t}) \tag{2.1}$$

or the matrix $\mathbf{\Theta}$ matrix that determined the observation y_{i,f_t} of the ith individual during its capture event, f, at time t (Appendix Table 5.1b):

$$y_{i,f_t} \sim Categorical(\mathbf{\Theta}_{i,f_t}) \tag{2.2}$$

We configured the observation process for the initial capture to assume perfect detection of the true state (the diagonal 1's in Appendix Table 5.1b), because the number of calves with each cow was determined during collaring.

For all subsequent observations of collared cows, we also assumed separate state- and observation-processes. The latent state process conditioned the state $z_{i,t}$ for the ith individual at time $t+1$ on the categorical distribution based on the matrix $\mathbf{Z}$, which held the transition probabilities between states (Eq. 2.3). We parameterized transition probabilities to estimate cow survival, calf survival, parturition probability, and twinning probability for appropriate transitions between states at times t and $t+1$ (Appendix Table 5.2a & 5.2b). Because most moose give birth from mid-May to mid-June, the first month of each study year (Aderman, 2014), we used an indicator function that constrained reproduction to the first month of every year. We defined this subset of t with only the first month of each year as the discrete set $t_p \equiv \{1, 13, ..., T-11\}$ (Appendix Table 5.2a & Eq. 2.3). Since survival processes occur year-round, we estimated survival probabilities for all months (Appendix Table 5.2b). As a result, for the first month, the state matrices were added together and estimated survival and reproductive probabilities, whereas for other months, the state process only estimated

survival probabilities (Eq. 2.3):

$$z_{i,t+1}|z_{i,t} \sim Categorical(\mathbf{Z}_{z_i,t} I(t \in t_p) + \mathbf{Z}_{z_i,t} I(t \notin t_p) \tag{2.3}$$

The observational likelihood for all observations after initial collaring (Eq. 2.4) estimated calf detection probability to account for disparities between calf states and the observations from radio-telemetry flights. The observation process conditioned the raw observation y of individual i at time t based on the matrix $\mathbf{O}$ (Appendix Table 5.2c) that allowed for imperfect calf detection:

$$y_{i,t}|z_{i,t} \sim Categorical(\mathbf{O}_{r,z_i,t}) \tag{2.4}$$

To analyze environmental, spatial, and individual effects with population parameters, we modeled cow survival (Eq. 2.5), calf survival (Eq. 2.6), parturition probability (Eq. 2.7), and twinning probability (Eq. 2.8) as functions of fixed and random effects. For our reproductive parameters – parturition and twinning – we lagged environmental conditions by one year to allow conditions during gestation to affect birth. Age as linear and quadratic effects were included in each model. To account for variable hunting management, we included GMU with 5 levels j as a random intercept for cow survival. To account for individual heterogeneity in demographic processes, we included random intercepts for each individual in each model. Finally, we included year as a random intercept for each function to produce annual estimates of each parameter. All models can be summarized as:

$$logit(\phi_{cw_{i,t}}) = \beta_0 + \beta_1 \times NDVI_t + \beta_2 \times WSI_t + \beta_3 \times age_i + \beta_4 \times age_i^2 + year_y + ind_i + GMU_j \tag{2.5}$$

$$logit(\phi_{ca_{i,t}}) = \beta_0 + \beta_1 \times NDVI_t + \beta_2 \times WSI_t + \beta_3 \times age_i + \beta_4 \times age_i^2 + year_y + ind_i \tag{2.6}$$

$$logit(\alpha_{i,t}) = \beta_0 + \beta_1 \times NDVI_{t-1} + \beta_2 \times WSI_{t-1} + \beta_3 \times age_i + \beta_4 \times age_i^2 + year_y + ind_i \tag{2.7}$$

$$logit(\gamma i, t) = \beta_0 + \beta_1 \times NDVI_{t-1} + \beta_2 \times WSI_{t-1} + \beta_3 \times age_i + \beta_4 \times age_i^2 + year_y + ind_i \tag{2.8}$$

We tested independence of each random effect between models by calculating pairwise Pearson's correlation coefficients (ρ) between all parameters for all individuals, using values of ρ <0.6 for independence. All ρ coefficients were below 0.6. We summarized annual parameter estimates using posterior means and 95% Bayesian credible intervals (BCI).

To assess annual productivity, we calculated calves per 100 cows, a metric used to inform moose management, using posterior distributions of annual estimates from parturition and twinning probabilities (Eq. 2.9):

$$cf100 = 100 \times ((\alpha_t \times (\gamma_t \times 2)) + (\alpha_t \times (1 - \gamma_t))) \tag{2.9}$$

We applied noninformative prior distributions to all coefficients, except cow survival which we expected to be high (Gaillard et al., 2000; Lowe and Aderman, 2014). We thus set the prior on the global intercept for cow survival to $Normal(2, 1)$, and $Normal(0, 2.25)$ for the intercept of other demographic parameters (Hooten and Hefley, 2019).

Coefficient priors for environmental conditions and age were set to $Normal(0, 1.5)$. All random effects ($year_y$, ind_i, GMU_j) were set to a $Normal(0, \tau)$ distribution, where hyperpriors for τ were set to a $Uniform(0, 5)$ distribution (Kèry and Schaub, 2011). The exception to this was τ for calf survival yearly random effects, which we set to $Uniform(0, 7)$ to accommodate higher-than-expected standard deviation.

To investigate temporal patterns in reproductive productivity, we also implemented posthoc generalized linear models (GLMs) in a frequentist framework between year and annual mean calves per 100 cows, and parturition and twinning probabilities. To maintain error propagation from the Bayesian multistate model, we conducted a GLM for each posterior distribution sample, and summarized slopes from all GLMs using the mean. We used a gamma GLM with a log link for calves per 100 cows, and quasibinomial GLMs with logit

links for parturition and twinning probabilities.

2.3.5 Model Implementation

To sample from posterior distributions of parameters, we conducted Markov chain Monte Carlo (MCMC) simulations in JAGS (Plummer, 2012) accessed using program R version 4.0.5 (R Core Team, 2021) utilizing the jagsUI package (Kellner, 2019). We ran the MCMC algorithm with 3 chains each consisting of 80,000 iterations with the first 20,000 discarded as burn-in, and used 100 iterations for sample adaptation. We assessed model convergence visually using traceplots and by ensuring that $\hat{R}$ (Brooks and Gelman, 1998) for each estimated parameter was less than 1.1 (Gelman and Hill, 2006; Kèry and Schaub, 2011).

We assessed the relationships of covariates in multistate submodels according to both the proportion of the MCMC sample from each marginal posterior distribution with the same sign as the mean, denoted as f (Kellner, 2019). We summarized slope coefficients from posthoc GLMs by similarly assessing the proportion of the resulting slope samples with the same sign as the mean. To summarize demographic parameters from the entire study time period, we reported posterior means and 95% credible intervals of all annual estimates.

2.4 Results

MCMC chains in all models converged such that traceplots appeared sufficiently mixed, and $\hat{R}$ values remained <1.1. The TNWR moose population exhibited variable population demographics between 1998 and 2020. Of all demographic parameters, annual cow survival varied the least between years (Appendix Table 5.3), and averaged 97.37% overall (Figure 2.2a). Calf survival varied the most between years (Appendix Table 5.3), and averaged 27.13% overall (Figure 2.2b). Parturition and twinning probabilities varied similarly (Appendix Table 5.3), and averaged 48.46% and 81.50%, respectively (Figure 2.2c & 2.2d). The

population averaged 87.68 calves per 100 cows (Supplemental Figure 5.1). Mean calf detection probability was 0.69 (95% BCI = 0.68, 0.71).

We found no temporal linear trends for NDVI and WSI for the study time period, but both correlated strongly with King Salmon, AK summer and winter temperatures, respectively, and King Salmon summer and winter temperatures increased linearly from 1970–2020 (Appendix Table 5.4). Additionally, NDVI and WSI correlated with PDO (Appendix Table 5.4), which phase shifted in a way that likely temporarily dampened NDVI and WSI linear increases (Kosaka and Xie, 2013).

Calf survival and twinning probabilities correlated strongly and positively with NDVI (Figure 2.3a & 2.3b), while cow survival correlated weakly and positively, and parturition did not correlate with NDVI (Appendix Table 5.5). The effect size of NDVI on calf survival was nearly three times that of twinning rate, where a 1.0 unit of NDVI increase resulted in an increase in calf survival from 3% to 50% and the same unit of NDVI increase resulted in an change in twinning rate from 73% to 92%.

Both calf survival and twinning probabilities correlated negatively with WSI (Figure 2.3c & 2.3d), but twinning probability correlated strongly and calf survival correlated weakly. Neither cow survival nor parturition probability correlated with WSI (Appendix Table 5.5). The effect sizes for calf survival and twinning rates were similar to each other (Appendix Table 5.4), where an increase in 6 WSI units resulted in calf survival decreasing from 36% to 6%, and in twinning rate decreasing from 95% to 70%.

All demographic parameters except calf survival related strongly with age as a linear term, and calf survival correlated weakly. Only parturition probability related with age as a quadratic term, albeit weakly. For both age terms, all parameters except twinning correlated

negatively (Appendix Table 5.5). Predicted parturition and twinning probability values using linear and quadratic terms from all MCMC iterations plateaued at approximately 10 years of age, while predicted cow survival plateaued until age 10, after which it started to decline. Calf survival decreased steadily with age (Figure 2.4).

Cow survival varied moderately across GMUs (Appendix Table 5.3), and comparisons between GMUs for cow survival revealed higher cow survival in 18G than all other GMUs. GMUs 18KA and Neither consistently had the lowest cow survival, while 17A and 17C had similar moderate cow survival probabilities (Table 2.1).

Individual random effects indicated varying levels of individual heterogeneity for each demographic parameter. Calf survival showed the highest amount of variation between individuals (sd = 2.67) (Figure 2.5), while twinning (sd = 0.75) and parturition (sd = 0.67) probabilities showed moderate variation. The least variation between individuals occurred in cow survival (sd = 0.27). Pairwise Pearson's correlation tests between parameters by individual indicated a lack of correlation between all random effects, where all but one pairwise correlation resulted in $|\rho| \leq 0.05$ (Appendix Table 5.6). The correlation between calf survival and parturition ($\rho = 0.17$) (Figure 2.5) was thus an outlier, but was still low enough that the parameters could be considered independent from one another. Pairwise Pearson's correlation tests between each individual's mean intercept and standard deviation for each parameter indicated negative, and substantially stronger correlations for survival ($\rho_{cowsurvival}$ = -0.38 & $\rho_{calfsurvival}$ = -0.41) than reproductive estimates ($\rho_{parturition} = 0.05$ & $\rho_{twinning} = 0.09$).

We found temporal trends for calves per 100 cows, and parturition probability, but not for twinning probability. Ninety-three percent of slope coefficients for calves per 100 cows over time fell below 0 and averaged -0.01, which equated to an average decrease of 1 calf

per 100 cows, per year. 94% of slope coefficients for parturition probability fell below 0 and averaged -0.02, which equated to an average parturition probability decrease of 1.2% per year, for any given moose. 54% of slope coefficients for twinning probability fell above 0, and averaged 0.00, indicating no change in twinning probability over time.

2.5 Discussion

We found similar relative mean values and variation of demographic rates compared to other ungulate and moose populations (Boer, 1992; Gaillard et al., 2000; Boertje et al., 2007), indicating good model function. Important correlations between the most variable demographic parameters (twinning and calf survival) and environmental conditions, and a strong relationship between those environmental conditions and warming in the region, point towards the hypothesis that alleviating environmental conditions over a long period of time played an important role in the moose population expansion into TNWR. Higher cow survival in areas with hunting moratoriums speaks to the influence human hunting pressure can have on population dynamics, and provides a possible explanation for what limited population growth while environmental conditions improved. While moose are highly mobile and adaptive to novel environments (Wattles et al., 2018; Groves et al., 2022), this study suggests that climate change, specifically the increase in vegetation productivity and decrease of winter severity, and changing hunting pressure abetted the rapid population growth of this sub-arctic species by improving population vital rates known to limit population growth (Gaillard et al., 2000; Gaillard and Yoccoz, 2003).

2.5.1 Environmental Effects on Demographic Parameters

Calf survival, though typically associated with lower elasticity toward population growth rate, is known to be one of the most temporally variable demographic rates for ungulates and thus one of the limiting factors of population growth (Gaillard et al., 2000; Gaillard and Yoccoz, 2003). We found that calf survival correlated strongest with vegetation pro-

ductivity (NDVI) (Figure 2.3 & Appendix Table 5.5), indicating that increasing NDVI was a driving factor behind the rapid moose population expansion in TNWR. The biological mechanism behind this pattern is likely one of improving calf and dam body condition with higher vegetation productivity; greater food quantity and, potentially, quality, allow dams to improve lactation rates before the calf weans from its mother, and provides ample nutrition for the calf as and after it weans (Festa-Bianchet et al., 1998; Ericsson et al., 2001). These factors likely combine to produce higher calf body mass by the end of fall, which has been shown to lead to higher overwinter survival in other cervids (Hurley et al., 2014; Loe et al., 2021). Positive effects of higher NDVI might also be attributed to greater vegetation cover for protection against predators, but this phenomenon has not been observed in ungulates. Additionally, we found a weak negative relationship between calf survival and winter severity (WSI), which has not been well documented. This pattern was observed during one severe winter in southcentral Alaska, when 81% of calf winter starvation during the study occurred over one snow-heavy season (Ballard et al., 1991). Lower calf survival in more severe winters in our study area likely occurred through the same mechanism, where high snow reduced mobility and increased physiological stress, and reduced food availability. Since calves have less robust fat reserves than adults, these stressful winters could have pushed them to starvation. This relationship was weak, however, and merits further investigation.

Evidence we found of bottom-up influence on calf survival from correlation with NDVI and WSI contradicts previous reports of dominant top-down effects (Ballard et al., 1990, 1991; Franzmann and Schwartz, 1998; Bertram and Vivion, 2002). The findings from a study that investigated calf survival before and after predator treatments may provide some insight for why our results contradict much of the literature. Keech et al. (2011) found that nonpredation calf mortality increased following wolf and bear reductions, and that calf survival was only then influenced by snow depth and temperature. Because predation pressure in TNWR is low (Aderman, 2014), it is likely that NDVI and WSI only affect survival

because overall predation pressure is low.

The high twinning probability average across all years indicated consistently high cow body condition (Franzmann and Schwartz, 1998; Boertje et al., 2007, 2019), but our results show that twinning probability increased in years with higher NDVI, and lower WSI (Figure 2.3 & Appendix Table 5.5). The relationship between habitat productivity and twinning rate has been well documented in the literature, where greater nutrient content across moose habitat facilitates higher body condition (Boer, 1992; Franzmann and Schwartz, 1998; Gaillard et al., 2000). Pregnant cows in good body condition are then more likely to birth twins. Although twinning probability in the study area remained high across all NDVI values relative to other populations (Boertje et al., 2007), the observed positive relationship between twinning and NDVI suggests that low summer vegetation productivity can limit recruitment in the following year.

The negative relationship we observed between twinning probability and winter severity has not, to our knowledge, been documented previously in moose, where multiple populations showed no correlation between snow conditions and twinning rates (Testa, 2004; Boertje et al., 2019). These studies, however, took place in the core of Alaskan moose distribution, and the fact that we did find correlation could be unique to our study area that exists at the current edge of moose ranges, where winter conditions may be harsher. Other studies have found that moose populations inhabiting the peripheries of their southern ranges react differently to environmental conditions than those in the core range (Ditmer et al., 2018; Ruprecht et al., 2020; Oates et al., 2021), and it may be similar for populations at the northern peripheries. The relationship between winter severity and recruitment has, however, been documented in grazing ungulates (Cosgrove et al., 2021). Because grazers paw through snow to access food, higher snow depth leads to caloric deficits by decreasing forage access and increasing physical exertion (Robinson and Merrill, 2012). Although moose are

browsers, a similar mechanism of caloric deficit might occur as pregnant females burn fat reserves moving through deep snow to access food. Excessive fat loss, perhaps unique to the extreme conditions moose occupy in TNWR, might decrease body condition, thereby reducing twinning probability.

We found limited to no influence of environmental conditions on cow survival or parturition rates (Appendix Table 5.5), which we expected given large herbivore life history that tends towards stable cow survival and pregnancy rates (Gaillard et al., 2000; Gaillard and Yoccoz, 2003). Interestingly, the limited influence we did find was a weak positive correlation between cow survival and NDVI (Appendix Table 5.5), which, considering how high elasticity is for adult survival in ungulate populations (Gaillard et al., 2000), could have major ramifications for improving population growth rates. Similar to the relationship we found with calf survival, this effect could exist due to low hunting pressure; contrary to most of the literature that shows adult mortality is primarily due to predation (Bertram and Vivion, 2002; Ballard et al., 1991; Testa, 2004), one study found that nutrition improved adult survival in a low-predator environment (Oates et al., 2021). This was, however, a weak relationship and should be further investigated.

Climate change, in the form of higher vegetation productivity and less severe winters, was thus likely a major driver of rapid moose population expansion in southwest Alaska, but not necessarily in the time period we studied. This is because we did not find that NDVI or WSI changed linearly over the 24-year study time period, but the population did (Aderman, 2014; Aderman et al., 2019). We did, however, find that both NDVI and WSI correlated significantly with winter and summer temperatures at a nearby long-term weather station, in King Salmon, AK (Appendix Table 5.4). Over five decades, these winter and summer temperatures increased significantly (Appendix Table 5.4), suggesting that, over a longer time period than our study, NDVI increased and WSI decreased. We might not have detected a

linear trend in WSI or NDVI in our study time period due to a multi-year oscillation of the Pacific Decadal Oscillation (PDO) that paused temperature increases worldwide (Kosaka and Xie, 2013). Considering NDVI and WSI correlated significantly with PDO (Appendix Table 5.4), a multi-year cooling event could have precluded the linear relationship we attempted in our analysis.

Ultimately, we found that elements of climate change explained variation in vital rates of the moose population in such a way that indicates that vegetation availability and winter conditions improved living conditions for moose since temperatures started warming in southwest Alaska. Conditions had clearly been amenable to low density moose populations at least in the eastern half of TNWR since the 1850s (Abercrombie et al., 1900), but our results suggest conditions improved steadily, which increased calf survival and twinning rates, which may have led to higher and more consistent population growth rates. The rapid population growth that began in the 1980s (Aderman, 2014) may be the result of a range boundary disequilibrium (Sexton et al., 2009), where improving TNWR habitat could have supported higher density moose populations, but some external factor prevented their growth.

2.5.2 Hunting

Differing cow survival rates by GMUs indicate human hunting pressure had a large influence on moose population expansion, and could have prevented growth despite improving conditions. The differences we found were in cow survival between GMU's, where cow survival was consistently highest in 18G, lowest in 18KA, and moderate and similar in 17C and 17A (Table 2.1). This indicates that human hunting pressure has the potential to alter important demographic rates, because managers and locals in 18G agreed upon a hunting moratorium in the mid-2000s that allowed moose populations to establish (Aderman, 2014). Following the moratorium, hunters avoided hunting collared cows (Aderman, unpublished data), thus potentially artificially overestimating cow survival. A hunting moratorium was

not established in 18KA, and cows there likely continually experienced high hunting pressure. Hunting in 17A and 17C was strongly monitored and controlled throughout the time period, thus explaining moderate cow survival levels. While we could not definitively establish hunting as a driver of vital rates, these differences clarify how human hunting pressure can have a substantial effect on ungulate populations and range expansion (Tape et al., 2016). Given that, anecdotally, hunting pressure diverted towards caribou when the Mulchatna caribou herd peaked in the mid-1990s (Valkenburg et al., 2003; Aderman, 2014), it seems likely that this diversion allowed human-induced low moose density populations to flourish in habitat that had rapidly been improving.

2.5.3 Age Effects

Our finding that age related strongly with nearly every demographic parameter suggested that age and environmental processes may affect the population separately; while we found environmental conditions affected some parameters, it still could not override intrinsic biological senescence. Inclusion of interaction terms in multistate submodels could support this interpretation, but we did not include such terms to reduce the model's complexity. Additionally, our results largely fell within expectations that adult and calf survival probabilities decreased as age increased (Boertje et al., 2019; Loison et al., 1999; Ericsson et al., 2001) and that twinning probability increased with age (Boertje et al., 2019). We were surprised, however, by the asymptotic relationship with twinning at older ages, and the strong negative relationship with parturition. While Boertje et al. (2019) found a similar increase in twinning probability with age, twinning probability in their study decreased and became more variable at older ages, whereas we found twinning probability peaked close to the average age, and stayed high. This might be because of the high nutritional plane that moose in TNWR inhabit, that keeps older parturient moose consistently able to birth twins.

We expected similar results with parturition as we did with twinning, especially con-

sidering results from other studies (Boertje et al., 2019) and earlier frequentist analysis of similar data that produced a similar relationship (Lowe and Aderman, 2014). Instead, we found a four-fold decrease in probability of parturition from the youngest to the average age followed by an asymptote to zero after age 10. One possible explanation for this largely undocumented result is that we were not able to reliably detect calves of middle-age to older cows during the first month of birth, which the multistate model used to estimated reproductive parameters. We think the relationship between calf detection and cow age exists either because older cows might be better at hiding their calves, or because calf mortality is higher for older cows (Ericsson et al., 2001). Considering Lowe and Aderman (2014) found results supported by ungulate literature using similar data, the former argument seems most likely. This is especially true given our results of imperfect calf detection probability, and given Lowe and Aderman (2014) were able to estimate parturition by incorporating calves detected with cows after the first month of calves' lives. Allowing the model to estimate reproduction outside of the parturient month might increase estimates of parturition probability for older cows, and is worth pursuing in future model versions. Either way, the unexpected decrease in parturition with age deserves more attention outside of this study.

2.5.4 Individual Heterogeneity

Often, analyses similar to ours assume all individuals react similarly to environmental and demographic pressures, but individuals are not all of equal quality. This individual heterogeneity has been documented in other mammal populations (Chambert et al., 2013; Badger et al., 2020), where high quality individuals are able to sustain high reproductive output regardless of environmental or demographic conditions, but average to low quality individuals are sensitive to external and internal stochasticity. We only found evidence that collared cows differed by calf survival (Figure 2.5 & Appendix Table 5.3), which indicates intrinsic differences in maternal care between cows. If maternal care can be divided between

providing sustenance and protecting from danger (e.g. predators, rivers, etc.), and if calves are more likely to be sensitive to maternal care when neonate predation is low (Gaillard et al., 2000), it would seem the differences between life-long calf survival in cows would be due to providing sustenance. However, a cow's success in feeding her calf is typically dependent on her body condition, and if there were large quality differences between individuals, we would also expect to see individual heterogeneity in twinning, which is subject to nutritional condition of cows (Franzmann and Schwartz, 1998). Our results thus challenge the idea that calf survival is sensitive to maternal care when predation is low (assuming, as we have, that predation was low throughout the study time period (Aderman, 2014)), and that the existence of calf survival heterogeneity is related to protecting calves from danger. Ultimately, more investigation is required to understand the dynamics we present here, especially given that individual heterogeneity can affect population growth (Barbraud and Weimerskirch, 2005; Chambert et al., 2013; Jenouvrier et al., 2015; Badger et al., 2020).

It is also interesting that we did not find large variation in individual reproductive parameters, given that twinning and parturition rates varied so much between years (Appendix Table 5.3) and that twinning has been reported to vary substantially for moose (Boer, 1992; Gaillard et al., 2000). A possible explanation is that the bottom-up effects on reproduction are so strong they affect all individuals unilaterally; when conditions are bad, it's bad for all individuals, and vice versa.

2.5.5 Posthoc Analysis

Posthoc analysis of productivity and reproductive outputs suggested that population growth rate is slowing over the study time period, likely due to decreasing parturition. We attribute the potential for declining growth rates to parturition because while calves per 100 cows and parturition probability decreased with time, twinning probability remained consistently high. Therefore, whatever is causing parturition to decline is likely causing produc-

tivity to decline. Since we didn't find a correlation between parturition and NDVI, and only a weak correlation between parturition and winter severity, which itself is decreasing with time (Callaghan et al., 2011), but we did find a negative relationship between parturition and age, the cause of parturition decline might lie in an aging population. This seems unlikely, however, as growing populations like moose in TNWR typically have a younger-skewed age structure. Another possibility is that the growing population is causing density-dependent effects on parturition, especially in eastern areas that might be approaching carrying capacity.

2.5.6 Conclusions

Our findings suggest that climate change played an important role in rapid moose population growth in southwest Alaska, but not necessarily over the last three decades. Years with improved summer and winter conditions improved certain demographic parameters, but the population increased despite a lack of trends in those same environmental conditions over our study time period. Differences we found in cow survival by GMUs, and correlations with summer and winter conditions support the hypothesis that human hunting pressure maintained moose at low densities while their habitat improved, until the neighboring irrupting Mulchatna caribou herd (Valkenburg et al., 2003) diverted hunting pressure away from moose (Aderman, 2014). The correlations we found also point towards further population increases, as further increases in temperatures will likely increase vegetation productivity in moose habitat (Frost et al., 2021; Macander et al., 2022), and decrease winter severity (Lader et al., 2020). Our study contributes to understanding how animals are expanding their northern ranges in response to climate warming (see Chen et al. (2011)), and highlights the need to understand how colonization by large herbivores like moose might affect the ecosystem's ability to respond to climate change (see Vuorinen et al. (2020)). The link we forged between our study and population growth, however, would be stronger if we took population abundance into account, as density dependence can have an overwhelming

effect on demographic parameters relative to effects from environmental conditions (Post and Stenseth, 1998; Boertje et al., 2019). A strength of the multistate model we used in this study is that it can be integrated with a state-space model that uses population counts to estimate annual abundance in an integrated population model (IPM) (see Schaub and Kery (2021)). The IPM could account for density-dependence in the effects of environmental conditions on population growth, and thus more definitively link climate change to population growth.

2.6 Acknowledgments

We thank the many pilots and observers who, over three decades, collected data for this project. We thank T. Harms and everyone in the Spring 2022 Scientific Writing course, and C. Mulder and K. Tape for helpful comments on drafts of the manuscript. This work was funded through the US Fish and Wildlife Service, the Luick Memorial Travel Fund, the Calvin J. Lensink Fellowship, and two Teaching Assistantships from the UAF Department of Biology. We acknowledge that this work took place on ancestral homelands of Yup'ik, and lower Tanana Dené lands, and are grateful for their stewardship of these lands since time immemorial. Any use of trade, firm, or product names is for descriptive purposes only and does not imply endorsement by the U.S. Government. The findings and conclusions in this article are those of the author(s) and do not necessarily represent the views of the U.S. Fish and Wildlife Service.

2.7 References

Abercrombie, W. R., E. F. Glenn, O. O. Howard, I. Petroff, P. H. Ray, W. P. Richardson, and E. H. Wells (1900). *Compilation of Narratives of Explorations in Alaska.* Number 1023. US Government Printing Office.

Aderman, A. (2014). Monitoring moose demographics at Togiak National Wildlife Refuge, southwestern Alaska, 1998-2013. *Togiak National Wildlife Refuge, Dillingham, Alaska.*, 1–25.

Aderman, A., N. Barten, and M. Higham (2019). Estimation of moose abundance using the geospatial population estimator combined with a sightability model on Togiak NWR; final project report. *Western Alaska Landscape Conservation Cooperative Project*, 1–16.

Alaska Climate Research Center (2022a). Precipitation normals. Available at https://akclimate.org/data/precipitation-normals/.

Alaska Climate Research Center (2022b). Temperature normals. Available at https://akclimate.org/data/air-temperature-normals/.

Badger, J. J., W. D. Bowen, C. E. den Heyer, and G. A. Breed (2020). Variation in individual reproductive performance amplified with population size in a long-lived carnivore. *Ecology 101*, e03024.

Ball, J. P., C. Nordengren, and K. Wallin (2001). Partial migration by large ungulates: Characteristics of seasonal moose *Alces alces* ranges in northern Sweden. *Wildlife Biology 7*, 39–47.

Ballard, W. B., S. D. Miller, and J. S. Whitman (1990). Brown and black bear predation on moose in southcentral Alaska. *Alces: A Journal Devoted to the Biology and Management of Moose 26*, 1–8.

Ballard, W. B., J. S. Whitman, and D. J. Reed (1991). Population dynamics of moose in south-central Alaska. *Wildlife Monographs*, 3–49.

Barbraud, C. and H. Weimerskirch (2005). Environmental conditions and breeding experience affect costs of reproduction in blue petrels. *Ecology 86*, 682–692.

Bellard, C., C. Bertelsmeier, P. Leadley, W. Thuiller, and F. Courchamp (2012). Impacts of climate change on the future of biodiversity. *Ecology Letters 15*, 365–377.

Bertram, M. R. and M. T. Vivion (2002). Moose mortality in eastern interior Alaska. *The Journal of Wildlife Management 66*, 747–756.

Boer, A. H. (1992). Fecundity of North American moose (*Alces alces*): a review. *Alces: A Journal Devoted to the Biology and Management of Moose*, 1–10.

Boertje, R. D., G. G. Frye, and D. D. Young (2019). Lifetime, known-age moose reproduction in a nutritionally stressed population. *Journal of Wildlife Management 83*, 610–626.

Boertje, R. D., K. A. Kellie, C. T. Seaton, M. A. Keech, D. D. Young, B. W. Dale, L. G. Adams, and A. R. Aderman (2007). Ranking Alaska moose nutrition: Signals to begin liberal antlerless harvests. *Journal of Wildlife Management 71*, 1494–1506.

Brooks, S. P. and A. Gelman (1998). General methods for monitoring convergence of iterative simulations. *Journal of Computational and Graphical Statistics 7*, 434–455.

Callaghan, T. V., M. Johansson, R. D. Brown, P. Y. Groisman, N. Labba, V. Radionov, R. G. Barry, O. N. Bulygina, R. L. H. Essery, and D. M. Frolov (2011). The changing face of arctic snow cover: A synthesis of observed and projected changes. *Ambio 40*, 17–31.

Chambert, T., J. J. Rotella, M. D. Higgs, and R. A. Garrott (2013). Individual heterogeneity in reproductive rates and cost of reproduction in a long-lived vertebrate. *Ecology and Evolution 3*, 2047–2060.

Chen, I. C., J. K. Hill, R. Ohlemüller, D. B. Roy, and C. D. Thomas (2011). Rapid range shifts of species associated with high levels of climate warming. *Science 333*, 1024–1026.

Christie, K. S., J. P. Bryant, L. Gough, V. T. Ravolainen, R. W. Ruess, and K. D. Tape (2015). The role of vertebrate herbivores in regulating shrub expansion in the Arctic: A synthesis. *BioScience 65*, 1123–1133.

Chubbs, T. E. and J. A. Schaefer (1997). Population growth of moose, *Alces alces*, in Labrador. *Canadian Field Naturalist 111*, 238–242.

Collins, G. (2003). Togiak National Wildlife Refuge earth cover classification. *Progress Report, U.S. Fish and Wildlife Service, Dillingham, Alaska*.

Cosgrove, C. L., J. Wells, A. W. Nolin, J. Putera, and L. R. Prugh (2021). Seasonal influence of snow conditions on Dall's sheep productivity in Wrangell-St Elias National Park and Preserve. *PloS one 16*, e0244787.

Ditmer, M. A., R. A. Moen, S. K. Windels, J. D. Forester, T. E. Ness, and T. R. Harris (2018). Moose at their bioclimatic edge alter their behavior based on weather, landscape, and predators. *Current Zoology 64*, 419–432.

Epstein, H. E., I. Myers-Smith, and D. A. Walker (2013). Recent dynamics of arctic and sub-arctic vegetation. *Environmental Research Letters 8*, 015040.

Ericsson, G., K. Wallin, J. P. Ball, and M. Broberg (2001). Age-related reproductive effort and senescence in free-ranging moose, *Alces alces*. *Ecology 82*, 1613–1620.

Festa-Bianchet, M., J.-M. Gaillard, and J. T. Jorgenson (1998). Mass-and density-dependent reproductive success and reproductive costs in a capital breeder. *The American Naturalist 152*, 367–379.

Franzmann, A. W. and C. C. Schwartz (1998). *Ecology and Management of the North American Moose* (1 ed.). Wildlife Management Institute.

Frost, G. V., U. S. Bhatt, M. J. Macander, A. S. Hendricks, and M. T. Jorgenson (2021). Is Alaska's Yukon–Kuskokwim Delta greening or browning? Resolving mixed signals of tundra vegetation dynamics and drivers in the maritime Arctic. *Earth Interactions 25*, 76–93.

Gaillard, J.-M., M. Festa-Bianchet, N. G. Yoccoz, A. Loison, and C. Toigo (2000). Temporal variation in fitness components and population dynamics of large herbivores. *Annual Review of Ecology and Systematics 31*, 367–393.

Gaillard, J.-M. and N. G. Yoccoz (2003). Temporal variation in survival of mammals: a case of environmental canalization? *Ecology 84*, 3294–3306.

Gelman, A. and J. Hill (2006). *Data analysis using regression and multilevel/hierarchical models*. Cambridge University Press.

Gorelick, N., M. Hancher, M. Dixon, S. Ilyushchenko, D. Thau, and R. Moore (2017). Google Earth Engine: Planetary-scale geospatial analysis for everyone. *Remote sensing of Environment 202*, 18–27.

Groves, P., D. H. Mann, and M. L. Kunz (2022). Prehistoric perspectives can help interpret the present: 14,000 years of moose (*Alces alces* l) in the Western Arctic. *Canadian Journal of Zoology*.

Hewison, A. J., J. P. Vincent, J. M. Angibault, D. Delorme, G. V. Laere, and J. M. Gaillard (1999). Tests of estimation of age from tooth wear on roe deer of known age: variation within and among populations. *Canadian Journal of Zoology 77*, 58–67.

Hooten, M. B. and T. J. Hefley (2019). *Bringing Bayesian models to life*. CRC Press.

Hurley, M. A., M. Hebblewhite, J.-M. Gaillard, S. Dray, K. A. Taylor, W. K. Smith, P. Zager, and C. Bonenfant (2014). Functional analysis of normalized difference vegetation index curves reveals overwinter mule deer survival is driven by both spring and autumn phenology. *Philosophical Transactions of the Royal Society B: Biological Sciences 369*, 20130196.

Jenouvrier, S., C. Péron, and H. Weimerskirch (2015). Extreme climate events and individual heterogeneity shape life-history traits and population dynamics. *Ecological Monographs 85*, 605–624.

Kaeuffer, R., C. Bonenfant, J. Chapuis, and S. Devillard (2010). Dynamics of an introduced population of mouflon *Ovis aries* on the sub-Antarctic archipelago of Kerguelen. *Ecography 33*, 435–442.

Kaji, K., H. Okada, M. Yamanaka, H. Matsuda, and T. Yabe (2004). Irruption of a colonizing sika deer population. *The Journal of Wildlife Management 68*, 889–899.

Keech, M. A., M. S. Lindberg, R. D. Boertje, P. Valkenburg, B. D. Taras, T. A. Boudreau, and K. B. Beckmen (2011). Effects of predator treatments, individual traits, and environment on moose survival in Alaska. *Journal of Wildlife Management 75*, 1361–1380.

Kellner, K. (2019). jagsui: A wrapper around 'rjags' to streamline 'jags' analyses. R package version 1.5.1.

Kèry, M. and M. Schaub (2011). *Bayesian population analysis using WinBUGS: a hierarchical perspective*. Academic Press.

Kielland, K. and J. P. Bryant (1998). Moose herbivory in taiga: effects on biogeochemistry and vegetation dynamics in primary succession. *Oikos*, 377–383.

Kosaka, Y. and S.-P. Xie (2013). Recent global-warming hiatus tied to equatorial Pacific surface cooling. *Nature 501*, 403–407.

Lader, R., J. E. Walsh, U. S. Bhatt, and P. A. Bieniek (2020). Anticipated changes to the snow season in Alaska: Elevation dependency, timing and extremes. *International Journal of Climatology 40*, 169–187.

Lebreton, J., J. D. Nichols, R. J. Barker, R. Pradel, and J. A. Spendelow (2009). Modeling individual animal histories with multistate capture–recapture models. *Advances in Ecological Research 41*, 87–173.

Loe, L. E., G. E. Liston, G. Pigeon, K. Barker, N. Horvitz, A. Stien, M. Forchhammer, W. M. Getz, R. J. Irvine, and A. Lee (2021). The neglected season: Warmer autumns counteract harsher winters and promote population growth in arctic reindeer. *Global Change Biology 27*(5), 993–1002.

Loison, A., M. Festa-Bianchet, J.-M. Gaillard, J. T. Jorgenson, and J.-M. Jullien (1999). Age-specific survival in five populations of ungulates: evidence of senescence. *Ecology 80*, 2539–2554.

Lowe, S. J. and A. R. Aderman (2014). Effects of capture on the reproductive performance of female moose. *Journal of Fish and Wildlife Management 5*, 157–166.

Macander, M. J., P. R. Nelson, T. Nawrocki, G. V. Frost, K. Orndahl, E. C. Palm, A. F. Wells, and S. J. Goetz (2022). Time-series maps reveal widespread change in plant functional type cover across arctic and boreal Alaska and Yukon. *Environmental Research Letters 17*(5), 054042.

Myers-Smith, I. H., B. C. Forbes, M. Wilmking, M. Hallinger, T. Lantz, D. Blok, K. D. Tape, M. Macias-Fauria, U. Sass-Klaassen, and E. Lévesque (2011). Shrub expansion in tundra ecosystems: dynamics, impacts and research priorities. *Environmental Research Letters 6*, 045509.

NOAA (2022). Pacific decadal oscillation (PDO). Available at https://www.ncei.noaa.gov/access/monitoring/pdo/.

Oates, B. A., K. L. Monteith, J. R. Goheen, J. A. Merkle, G. L. Fralick, and M. J. Kauffman (2021). Detecting resource limitation in a large herbivore population is enhanced with measures of nutritional condition. *Frontiers in Ecology and Evolution 8*.

Plummer, M. (2012). JAGS version 3.4.0 user manual.

Post, E. and M. C. Forchhammer (2002). Synchronization of animal population dynamics by large-scale climate. *Nature 2002 420:6912 420*, 168–171.

Post, E. and N. C. Stenseth (1998). Large-scale climatic fluctuation and population dynamics of moose and white-tailed deer. *Journal of Animal Ecology 67*, 537–543.

Potter, C. and O. Alexander (2020). Changes in vegetation phenology and productivity in Alaska over the past two decades. *Remote Sensing 12*, 1546.

R Core Team (2021). R: A language and environment for statistical computing.

Robinson, B. G. and E. H. Merrill (2012). The influence of snow on the functional response of grazing ungulates. *Oikos 121*, 28–34.

Rosa, K., C. Dale, J. Purcell, M. Wood, and J. Snook (2020). Inuit knowledge and values of moose in Nunatsiavut Torngat Wildlife and Plants Co-Management Board. *Torngat Wildlife, Plants and Fisheries Secretariat Series*, 1–70.

Ruprecht, J. S., D. N. Koons, K. R. Hersey, N. T. Hobbs, and D. R. MacNulty (2020). The effect of climate on population growth in a cold-adapted ungulate at its equatorial range limit. *Ecosphere 11*, e03058.

Schaub, M. and M. Kery (2021). *Integrated population models: theory and ecological applications with R and JAGS*. Academic Press.

Secretariat, A. (2021). Arctic climate change update 2021: Key trends and impacts. *Arctic Monitoring and Assessment Programme*, 1–16.

Sexton, J. P., P. J. McIntyre, A. L. Angert, and K. J. Rice (2009). Evolution and ecology of species range limits. *Annual Review of Ecology, Evolution and Systematics 40*(1), 415–436.

Sturm, M., C. Racine, and K. Tape (2001). Increasing shrub abundance in the Arctic. *Nature 411*, 546–547.

Sweanor, P. Y. and F. Sandegren (1989). Winter-range philopatry of seasonally migratory moose. *Journal of Applied Ecology 26*, 25–33.

Tape, K. D., J. A. Clark, B. M. Jones, S. Kantner, B. V. Gaglioti, G. Grosse, and I. Nitze (2022). Expanding beaver pond distribution in arctic Alaska, 1949 to 2019. *Scientific Reports 12*, 1–9.

Tape, K. D., D. D. Gustine, R. W. Ruess, L. G. Adams, and J. A. Clark (2016). Range expansion of moose in arctic Alaska linked to warming and increased shrub habitat. *PLoS ONE 11*.

Tape, K. D., B. M. Jones, C. D. Arp, I. Nitze, and G. Grosse (2018). Tundra be dammed: Beaver colonization of the Arctic. *Global Change Biology 24*, 4478–4488.

Tape, K. E. N., M. Sturm, and C. Racine (2006). The evidence for shrub expansion in northern Alaska and the pan-Arctic. *Global Change Biology 12*, 686–702.

Terskaia, A., R. J. Dial, and P. F. Sullivan (2020). Pathways of tundra encroachment by trees and tall shrubs in the western Brooks Range of Alaska. *Ecography 43*, 769–778.

Testa, J. W. (2004). Population dynamics and life history trade-offs of moose (*Alces alces*) in south-central Alaska. *Ecology 85*, 1439–1452.

Testa, J. W. and G. P. Adams (1998). Body condition and adjustments to reproductive effort in female moose (*Alces alces*). *Journal of Mammalogy 79*, 1345–1354.

Valkenburg, P., R. A. Sellers, R. C. Squibb, J. D. Woolington, A. R. Aderman, and B. W. Dale (2003). Population dynamics of caribou herds in southwestern Alaska. *Rangifer 23*(5), 131–142.

Viereck, L. (1979). Characteristics of treeline plant communities in Alaska. *Holarctic Ecology 2*, 228–238.

Vuorinen, K. E. M., A. L. Kolstad, L. D. Vriendt, G. Austrheim, J. Tremblay, E. J. Solberg, and J. D. M. Speed (2020). Cool as a moose: How can browsing counteract climate warming effects across boreal forest ecosystems? *Ecology 101*, e03159.

Walsh, J. E. and B. Brettschneider (2019). Attribution of recent warming in Alaska. *Polar Science 21*, 101–109.

Wattles, D. W., K. A. Zeller, and S. DeStefano (2018). Range expansion in unfavorable environments through behavioral responses to microclimatic conditions: Moose (*Alces americanus*) as the model. *Mammalian Biology 93*, 189–197.

Zhou, J., L. Prugh, K. D. Tape, G. Kofinas, and K. Kielland (2017). The role of vegetation structure in controlling distributions of vertebrate herbivores in arctic Alaska. *Arctic, Antarctic, and Alpine Research 49*, 291–304.

Zhou, J., K. D. Tape, L. Prugh, G. Kofinas, G. Carroll, and K. Kielland (2020). Enhanced shrub growth in the Arctic increases habitat connectivity for browsing herbivores. *Global Change Biology 26*, 3809–3820.

2.8 Figures

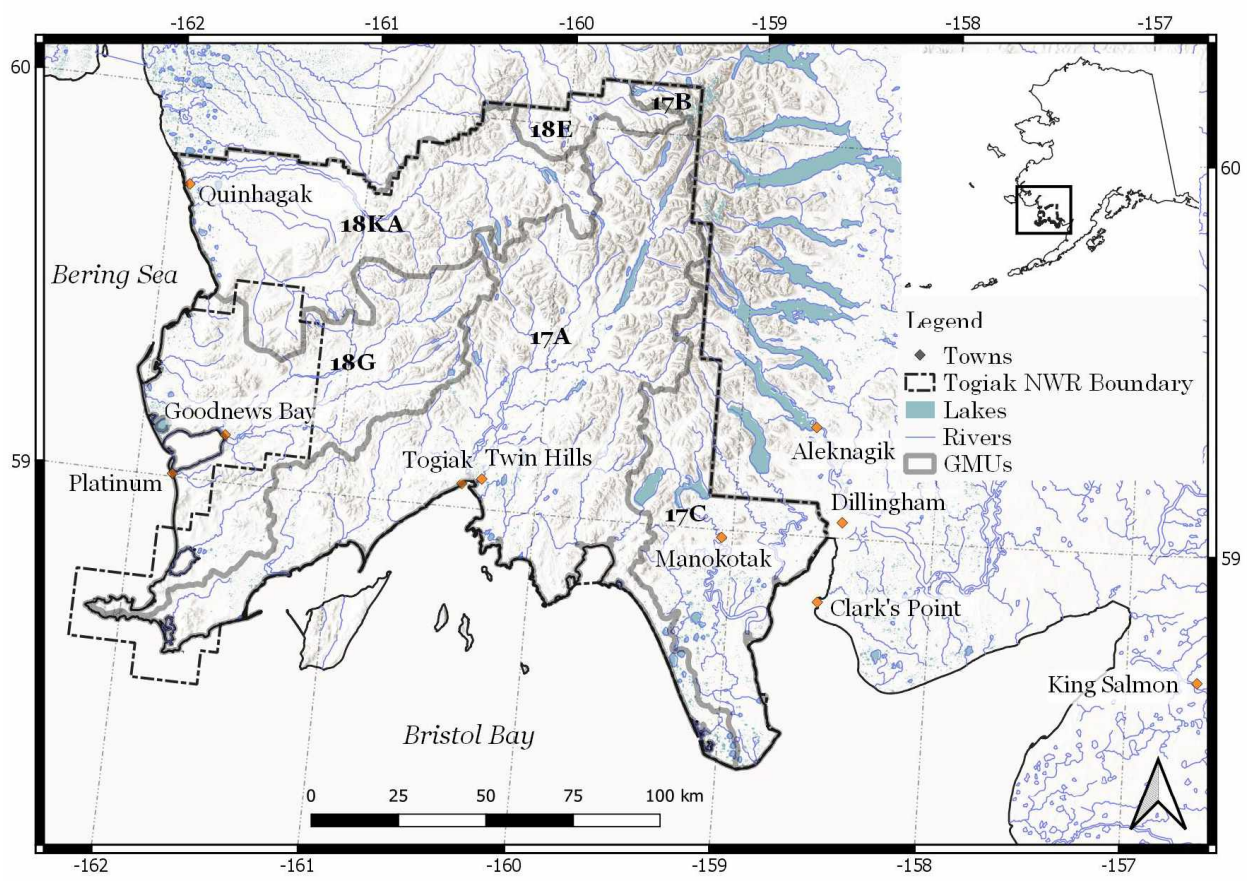

Figure 2.1: Togiak National Wildlife Refuge (TNWR) boundary and Game Management Units (GMUs) in which radio telemetry was conducted.

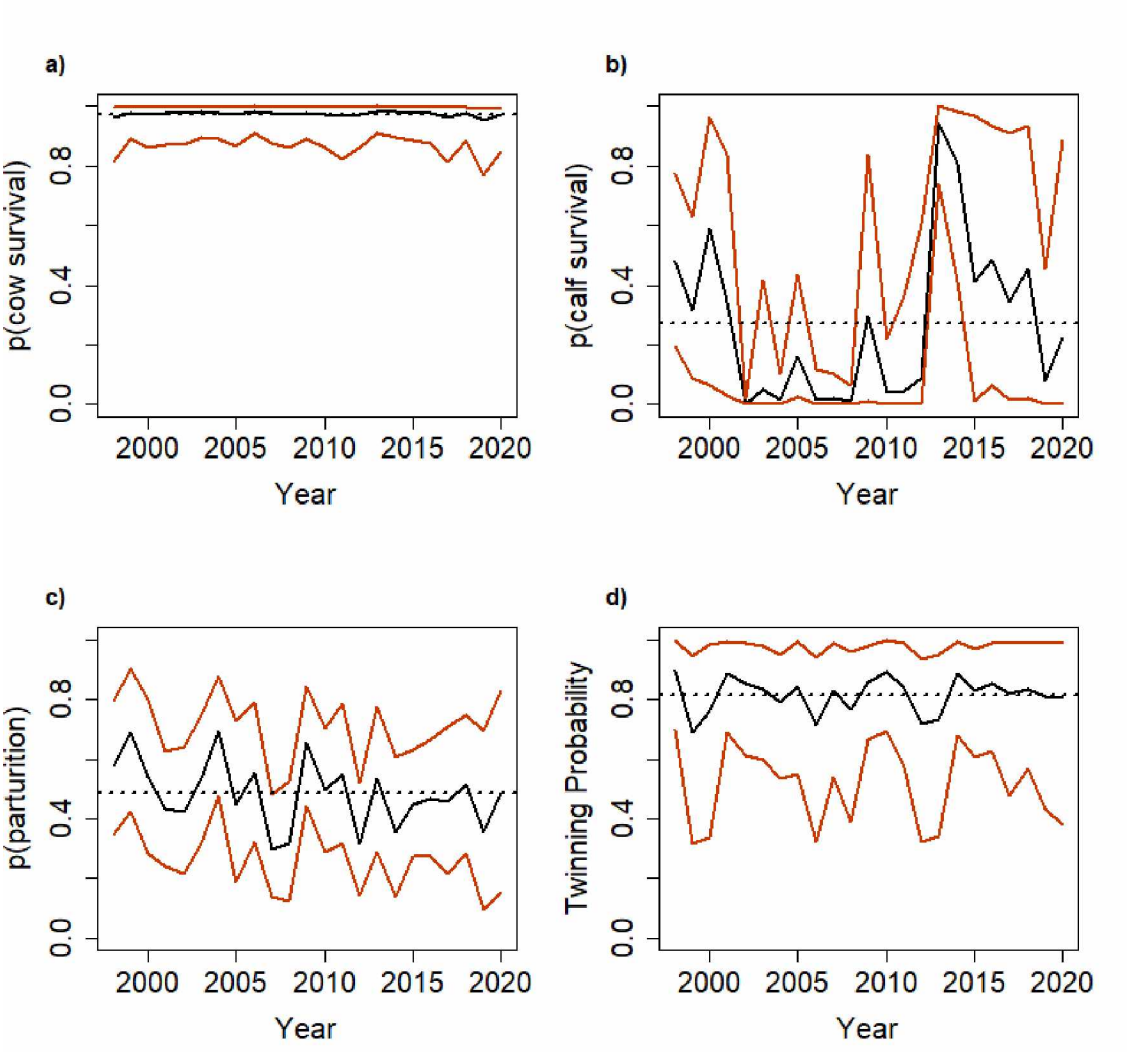

Figure 2.2: Annual estimates of demographic parameters from the random effect of year in all logistic regressions, including a) cow survival probability (note constrained y-axis), b) calf survival probability, c) parturition probability, and d) twinning probability. Solid black lines indicate posterior annual means, red lines indicate upper and lower 95% Bayesian Credible Intervals, and dotted lines indicate global posterior means.

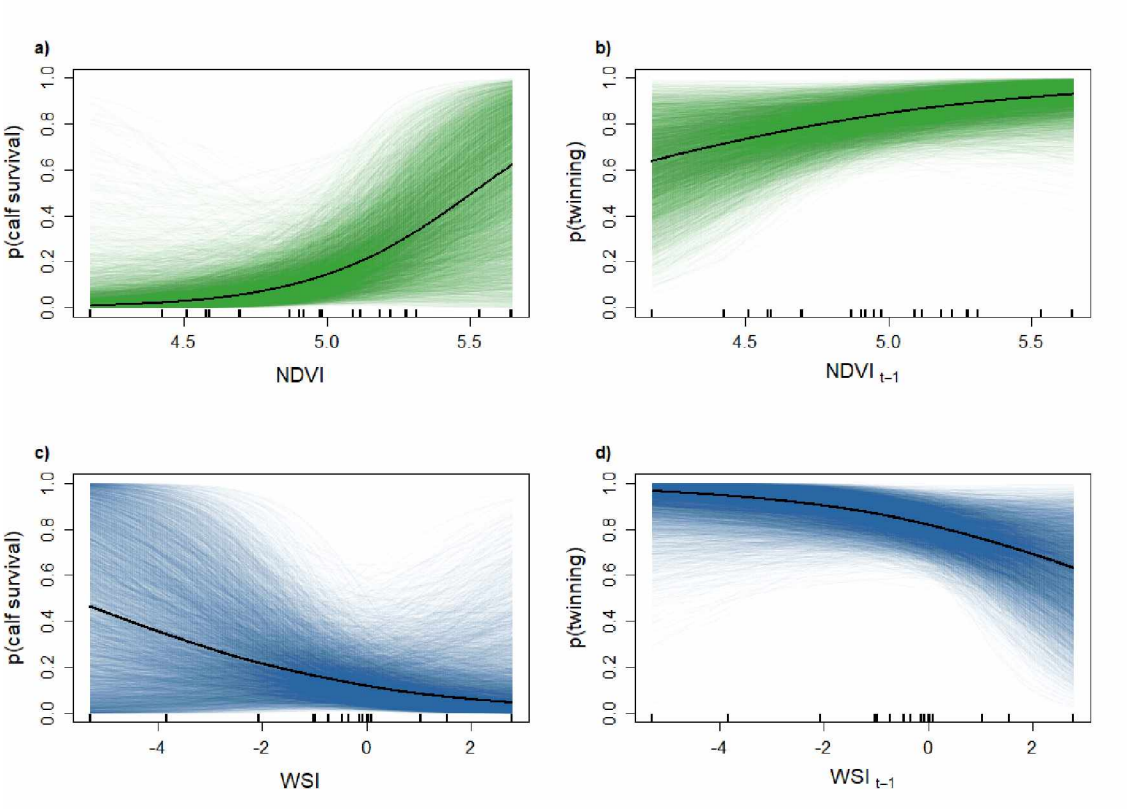

Figure 2.3: Fitted logistic relationships between demographic parameters and environmental covariates showed strong correlation for: a) annual summer NDVI and calf survival probability, b) previous summer's NDVI and the twinning probability, c) winter severity and calf survival probability, d) previous winter severity and twinning. Individual lines are posterior realizations from each MCMC sample, bold black lines represent the median coefficient value, and black tick marks along the x-axis show the spread of covariate values.

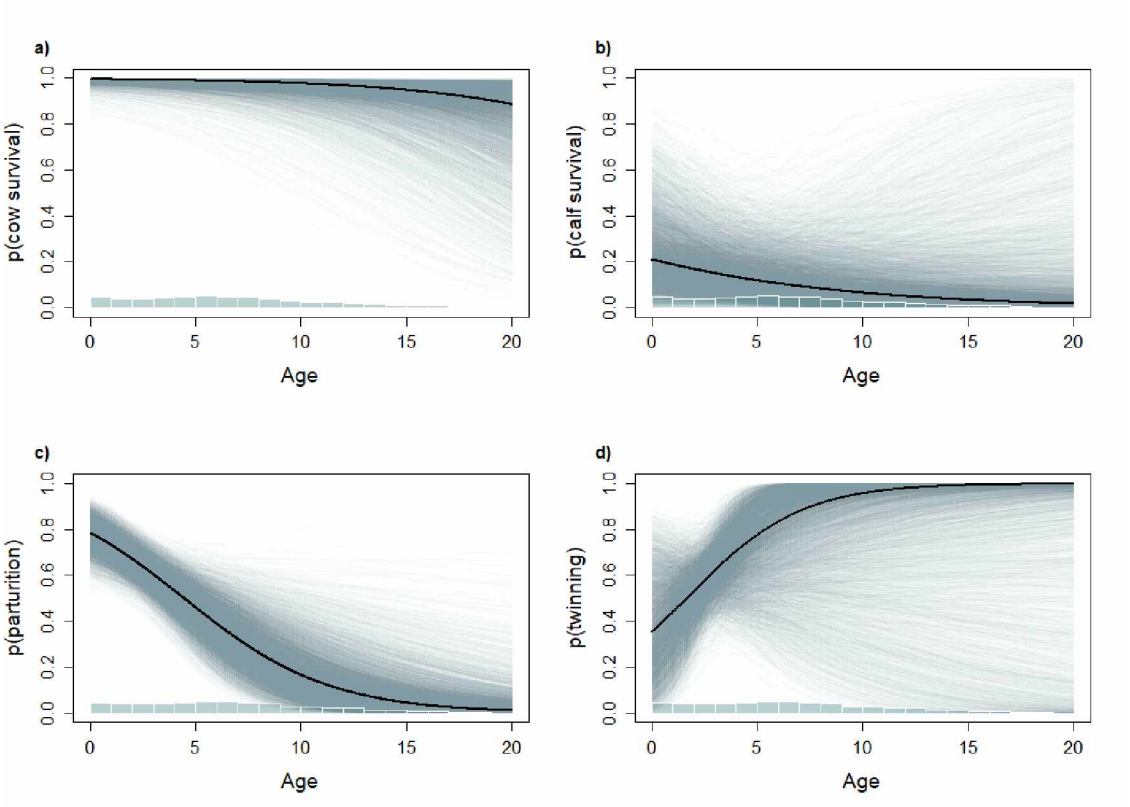

Figure 2.4: Fitted logistic relationships between demographic parameters and centered and scaled age covariates (linear and quadratic coefficients) that showed: a) negative linear relationship between age and cow survival probability, b) quadratic relationship between age and calf survival probability, c) negative quadratic relationship between age and parturition probability, d) positive relationship between age and twinning probability. Individual lines are individual samples of coefficients from all 60,000 iterations of the model, bold black lines represent the mean coefficient values, and mini histograms along the x-axis represent the frequency of ages across all years (all histograms are identical).

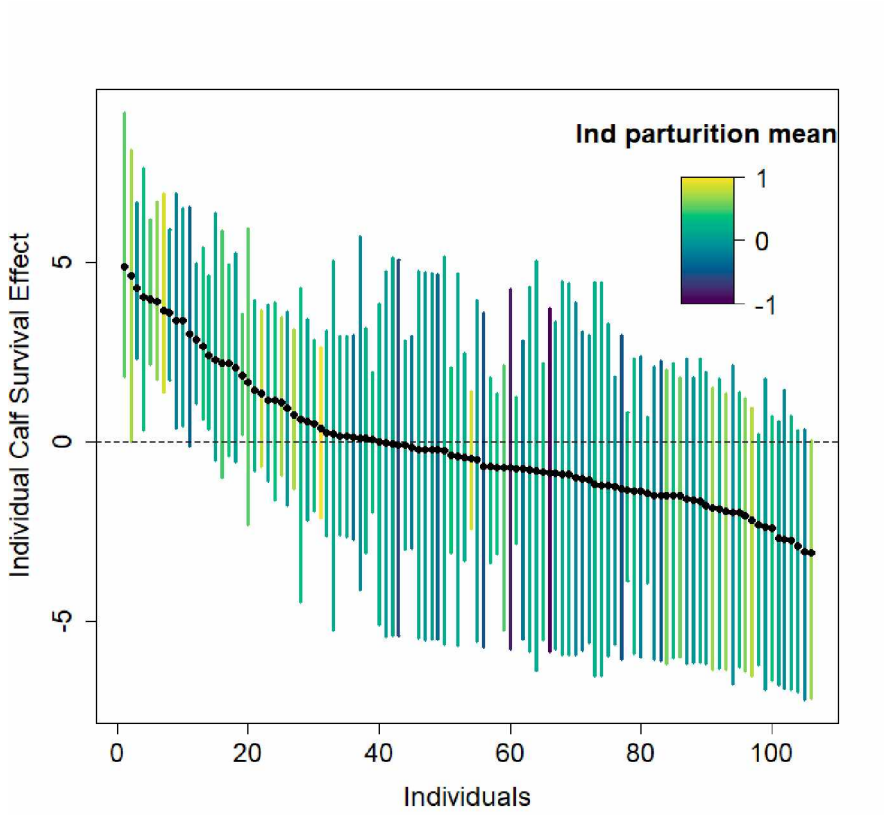

Figure 2.5: Caterpillar plot of each individual's estimated lifetime effect on calf survival. Black dots represent posterior means and bars span the 95% credible interval. Bars are colored by the individual's estimated effect on parturition. Units are probability in logit space.

2.9 Tables

Table 2.1: Comparison of cow survival means by Game Management Unit (GMU). We included GMU as a random intercept variable in models of cow survival to account for hunting management history. Means refer to the mean of the posterior distribution resulting from the difference of the posterior distributions of respective GMUs. f refers to the proportion of the posterior distribution with the same sign as the mean.

GMU Comparison	Difference	f
17A vs 17C	0.08	0.59
17A vs 18G	-0.56	0.90
17A vs 18KA	0.68	0.84
17A vs Neither	0.45	0.88
17C vs 18G	-0.65	0.84
17C vs 18KA	0.60	0.75
17C vs Neither	0.37	0.71
18G vs 18KA	1.25	0.94
18G vs Neither	1.02	0.97
18KA vs Neither	-0.23	0.62

Chapter 3: Demographic drivers of population growth for a colonizing sub-arctic ungulate[2]

3.1 Abstract

The demographic buffering hypothesis (DBH) states that natural selection minimizes temporal variation for high sensitivity vital rates, at the expense of higher variability in lower sensitivity vital rates. While this hypothesis has been upheld numerous times, it is still unclear which vital rates - those that vary, or have high sensitivity - actually impact observed population growth rates. Clarifying this discrepancy has implications for conservation and management of long-lived vertebrates, as conservation efforts often focus on improving high sensitivity vital rates. We conducted transient life table response experiments (tLTRE) with an integrated population model (IPM) that merged count and telemetry data of a rapidly increasing moose (*Alces alces*) population in southwest Alaska from 1997–2020. Our objectives were to better understand reasons for the colonization of moose in the area, and to further uncover patterns of impacts of vital rates on population growth rate for long-lived vertebrates. Overall, adult survival varied the least and exhibited the highest sensitivity, in line with the DBH, but contributed very little to variance in population growth rate. Calf survival varied the most, and contributed the most to variance in population growth rate. Our results suggest that an outcome of variability reduction in a vital rate, barring high predation or direct anthropogenic issues, is that the most variable vital rate subsequently drives population dynamics. Additionally, environmental conditions affecting calf survival have limited population growth over our study time period, and may have limited colonization when the population struggled to establish itself. More work is needed to understand factors influencing calf survival, and whether contributions from vital rates change as abundance increases.

[2]Zavoico, VS, JM Eisaguirre, SM Crimmins, AA Aderman, GG Frye, MA Cobb, MS Lindberg. 2023. Demographic drivers of population growth for a colonizing sub-arctic ungulate. Prepared for submission: Journal of Animal Ecology.

3.2 Introduction

Populations generally benefit from stability (Gillespie, 1977), and have evolved to combat environmental variation by enhancing fitness in a myriad of ways. The result is a life history strategy uniquely fit to certain climates and habitats. Driven by naturally occurring environmental stochasticity, it is thought that species must trade off stability in some life history components to maintain those most important to their fitness. This trade-off is central to the demographic buffering hypothesis (DBH) (Pfister, 1998), which predicts an inverse relationship between the variance of a demographic rate and its potential impact on population growth rate (i.e. sensitivity/elasticity). Not all species 'sacrifice' the same vital rates, however, and which vital rates are traded off depends on the life history strategy of the species (Gaillard and Yoccoz, 2003) and how close a population is to carrying capacity (Eberhardt, 2002). Understanding inherent demographic pathways that most influence population dynamics for species can better inform conservation and management decisions (Zipkin and Saunders, 2018; Sher, 2022).

Long-lived species evolved a strategy prioritizing adult survival over reproduction, as foregoing reproduction in bad years can lead to continual recruitment in future years (Eberhardt, 2002; Gaillard and Yoccoz, 2003). An extreme example of this phenomenon is white-tailed deer abandoning freshly birthed fawns after a winter of nutritional stress; even with milk in the udder, females prioritized regaining body mass after the stressful winter to ensure future reproduction opportunities (Langenau Jr and Lerg, 1976). Juvenile survival typically has the lowest sensitivity of any vital rate, and thus most long-lived species follow this example of trading off juvenile survival for adult survival. As a result, and in line with the DBH, juvenile survival generally has the highest variance, though there are some exceptions (e.g. Rotella et al., 2012). For polytocous species, who may give birth to multiple young simultaneously, birth rate has lower variance than the rate at which they give birth to two or more offspring (Boer, 1992; Gaillard et al., 2000). However, neither patterns in variance for lower

sensitivity vital rates, nor their relation to population density or environmental conditions, have been exhaustively explored.

While tenets of the DBH are established, what is not as well known is how outcomes of the DBH actually affect population growth. Pfister (1998) stated that, because adult survival has the highest sensitivity, any variation in that vital rate should drive population growth rate. However, sensitivity only measures potential effects of vital rates on population growth rate (Caswell, 2000). Most studies since that of Pfister (1998) (see life table response experiments (LTRE) (Caswell, 1989) and life stage analysis (LSA) Wisdom et al. (2000)), calculated sensitivity using asymptotic growth rate, a process that ignores variance in population structure and vital rates occurring in changing environments (Tuljapurkar, 1990). To combat this, recently developed transient life table response experiments (tLTRE) measure actual impacts on growth rate. tLTRE analysis accomplishes this by estimating contributions of variance from vital rates and components of population structure to realized population growth rate, thus accounting for environmental stochasticity (Koons et al., 2016, 2017). Therefore, tLTRE analysis requires population structure and vital rate data for coinciding time periods, which can be difficult to acquire for vertebrate populations. Integrated population models (IPM) are well suited to accompany tLTRE analysis, as they can be used to simultaneously estimate time-varying vital rates, population structure, abundance, and population growth rates using count and vital rate data (Brooks et al., 2004; Schaub et al., 2007; Schaub and Abadi, 2011; Schaub and Kery, 2021). IPMs can handle gaps in datasets, and be conducted in a Bayesian framework, which allows for complete error propagation for derived parameters (Maunder and Punt, 2013).

We conducted tLTRE analysis with an IPM that incorporated count and telemetry data from a rapidly expanding moose (*Alces alces*) population in southwest Alaska. This particular moose population, in Togiak National Wildlife Refuge (TNWR), existed at low densities

from at least the 1850s (Abercrombie et al., 1900) to the 1980s, when it expanded from approximately 12 individuals, to over 3,500 in 2017 (Aderman et al., 2019), for largely unknown reasons. Current hypotheses include: 1) immigration from the east, 2) collaborative efforts between TNWR biologists and local residents to reduce illegal harvest, 3) availability of the Mulchatna Caribou Herd for subsistence needs during the irruption in the 1990s (Valkenburg et al., 2003), and 4) high quality and quantity of forage habitat (Aderman, 2014) likely the result of rapid ecological shift caused by climate change (Walsh and Brettschneider, 2019; Potter and Alexander, 2020; Frost et al., 2021; Macander et al., 2022). We used tLTRE analysis to uncover demographic drivers of the moose population in TNWR, which can both clarify reasons for the recent expansion, and improve understanding of demography of long-lived vertebrates.

3.3 Methods

3.3.1 Study Area

We analyzed radio telemetry and count data collected in and around Togiak National Wildlife Refuge (TNWR) in southwest Alaska, USA. The study area comprises 21,063 km^2 and includes various hunting management plans according to Game Management Units (GMUs). Portions of GMUs 17A, 17C, 17B, 17E and 18 are located in the study area, although we omitted 17B and 17E and partitioned GMU 18 into two portions: 18-Kanektok-Arolik (18KA) and 18-Goodnews (18G) (Figure 3.1) to accommodate the count data collection process. TNWR is in a transitional climate zone, where both maritime and continental influences impact weather patterns, depending on Bering Sea sea ice extent. Average summer temperature in King Salmon, AK, the closest long-term weather station (Figure 3.1) is 12.8°C (1991–2020), and average winter temperature is -7°C (Alaska Climate Research Center, 2022b). Annual average precipitation is 54.5cm (1991–2020) (Alaska Climate Research Center, 2022a). TNWR is typically colder, receives more snow, and has a more durable snowpack than King Salmon (Aderman, unpublished data).

Vegetation in TNWR transitions from alpine tundra in central mountains to upland shrubs on lower slopes, to lowland and coastal tundra communities at sea level. Numerous lakes and rivers support extensive riparian communities that host productive deciduous shrubs and trees, and far eastern valleys include mixed boreal forests. Generally, vegetation productivity and biomass decrease from east to west (Viereck, 1979). Caribou (*Rangifer tarandus*) from the Mulchatna and Nushagak Pensinsula herds share similar territories with moose, and are subject to human and natural hunting pressure. Both ungulates are preyed on by wolves (*Canis lupus*), coyotes (*Canis latrans*), wolverines (*Gulo gulo*) and brown bears (*Ursus arctos*), though predation levels are unknown and thought to be low (Aderman, 2014).

3.3.2 Data Collection

3.3.2.1 Count data

Moose counts occurred in fall or winter from 1981–2019 using a minimum count approach. Each GMU was divided into different-sized Sample Units (SUs) that followed topographic features. Up to four fixed-wing aircraft worked together to survey each GMU, and one to two primary observers and the pilot (a secondary observer) systematically counted moose 100–200m above ground level on flight paths that differed according to terrain; observers flew parallel transects spaced 0.4 km apart in flat terrain, but deviated from this pattern to follow riparian or altitudinal corridors in mountainous terrain. Search intensity varied between SUs depending on the amount of habitat and the number of moose encountered. Observers delineated moose to age (calf or adult) and sex (males with antlers or females with calves), though the latter was difficult to impossible in late winter when most males had lost their antlers. Counts were conducted once or twice a year per GMU, but at varying intervals in between years according to aircraft and observer availability, and weather conditions; there are frequent data gaps between minimum counts for GMUs.

From 2016–2019, Aderman et al. (2019) conducted sightability surveys during counts in TNWR by locating collared or unique individuals (e.g. blonde coat, single antler) prior to the count, then determining whether observers without knowledge of unique individuals' locations saw these animals during the count. Detection probabilities were thus calculated according to sex and snow cover.

As most counts were conducted in late-winter, we eliminated all fall counts and used detection probability for 100% snow cover, which occurred for most late-winter counts in late-winter.

3.3.2.2 Telemetry Data

From 1998–2020, TNWR regularly fitted female adult, yearling, and calf moose with VHF radio collars (Telonics Inc, Mesa, Arizona, USA) equipped with a motion-sensitive mortality switch. VHF collars were replaced when moose lived long enough for collar batteries to die, and new individuals were collared every ~5 years to maintain sufficient sample size and a representative age distribution. Observers used fixed-wing aircraft to locate and determine calf association for each cow, and attempted to locate each individual once per month, but concentrated efforts during birthing months (May–June), the fall (November) and late winter (February–March). Many individuals were not observed monthly, however, either because monthly flights did not occur, or because telemetry signals were not detected during flights. When observers heard a mortality signal, they located the individual as soon as possible to confirm mortality. We calculated day of death as the median date in between the last live, and the first dead observation. Dates were recorded as day-of-year with respect to the first day of parturition (May 14) (Aderman, 2014).

3.3.3 Data Analysis: Integrated Population Model (IPM)

We built a stage-structured integrated population model with two age classes (Figure 3.2) to estimate GMU and TNWR-wide population abundance, adult and calf survival, and parturition and twinning rates, while accounting for imperfect detectability in the recapture and count observation processes. The model allows combining count and telemetry data into a joint likelihood to estimate parameters. Both models followed the state-space model formulation that comprises state and observation equations. While the state equations describe the dynamics of true, but unknown latent states, the observation equation links the observed data with the state process, assuming observation error. Here, we first describe the submodels for the two datasets shown in Figure 3.3, and then describe the Bayesian implementation of the model.

3.3.3.1 Likelihood for the population count data

For population count data, we used stochastic equations to describe the state process for the two age classes we had appropriate data for: calves and adults. While yearling moose tend to have lower survival and reproductive rates than adults (Gaillard et al., 2000), we did not have data to explicitly model yearling demographic rates, and thus treated yearling moose as adult moose. Since population counts were conducted shortly before birth, we formulated the likelihoods in a pre-birth pulse population model framework. This involved using the count from year t (t=1,...T, where T = 24), shortly before birth began in year *t+1*, and the demographic rates calculated for year *t+1* to estimate population abundance in year *t+1*. We thus formulated the state equations for N_{ca}, calves, and N_{ad}, adults in year t and GMU i (i=1,...,I, where I = 5), as:

$$N_{ca_{t+1,i}} \sim Poisson(N_{ad_{t,i}} * 0.5 * f_{t+1} * \phi_{ca_{t+1}}), \tag{3.1}$$

$$N_{ad_{t+1,i}} \sim Binomial(N_{ca_{t,i}} + N_{ad_{t,i}}, \phi_{cw_{t+1}}), \tag{3.2}$$

where ϕ_{ca} is apparent survival probability of calves in a year *t+1*, and ϕ_{cw} is the apparent survival probability for cows more than one year of age for a year *t+1*. N_{ca} and N_{ad} refer to the latent true abundances of calves and adults estimated from minimum counts in year t. We note here an important assumption of Eq. 3.2 that cow survival rates are representative of all moose survival rates. This exists because counts did not account for sex, and we only had radiocollar data for cows. This assumption may be problematic as bulls typically have lower annual survival rates than cows (Franzmann and Schwartz, 1998), but was not an assumption we knew how to account for. The symbol f_t represents the fecundity in year t that we calculated as a function of parturition rate (α), twinning rate (γ), and singleton rate (1-γ):

$$f_t = ((\alpha_t * (\gamma_t * 2)) + (\alpha_t * (1 - \gamma_t)) \tag{3.3}$$

which we multiplied by 0.5 (Eq. 3.1) to reflect the assumption of an even population sex ratio.

The observation equation (Eq. 3.4) allowed us to account for imperfect detection of moose during counts, and linked the observed population count, y, to true population size, divided into calf and adult proportions. We formulated the observation process as a binomial distribution:

$$y_t \sim Binomial(N_{calf_t} + N_{adult_t}, p_{count}) \tag{3.4}$$

Using a binomial distribution for the observation process allowed us to use the sightability study that estimated an 84% detection probability for any moose in full snow cover (Aderman et al., 2019). We denoted the likelihood of the population count data as:

$$L_{count} = [y|\phi_{ca}, \phi_{cw}, f, N] \tag{3.5}$$

3.3.3.2 Likelihood for the telemetry data

For telemetry data, we used a multistate model that estimated calf and cow survival, parturition and twinning probabilities, and calf detection probability using repeated observations of radio-collared cows across TNWR. We used the same state-space formulation and Likelihood ($L_{telemetry}$) in the IPM as in the multistate model in Chapter 2. For more details on the formulation of the multistate model, see the Model Framework section of the Methods section in Chapter 1 (page 17).

3.3.3.3 Joint Likelihood for the IPM

We assumed independence of the two ($L_{count}, L_{telemetry}$) likelihoods, though count data included collared individuals. Despite this apparent violation of the independence assumption, IPMs have been shown to be robust to minor dependencies between datasets (Abadi et al., 2010). The joint likelihood of the IPM was therefore the product of the likelihoods for the two datasets:

$$L_{IPM}(z, y|\phi_{cw}, \phi_{ca}, \alpha, \gamma, N_{ad}, N_{ca}, p_{calf}, p_{count}) = L_{telemetry} \times L_{count}. \tag{3.6}$$

The advantage of analyzing the two datasets simultaneously in an integrated framework was that it allowed parameters derived explicitly from each model – count data from the population model, and demographic rates from the multistate model – to simultaneously inform each other. This both increases precision of parameters and allows for proper error propagation throughout the model (Schaub and Abadi, 2011).

3.3.3.4 Derived Quantities

To collect additional measures of population dynamics, we created additional quantities within the IPM derived deterministically from stochastic parameters. This included the total annual abundance of each GMU ($N_{tot,i}$) and all of TNWR (N_{tot}) by adding up annual N_{ca}

and N_{ad} estimates of all GMUs. We also calculated the realized population growth rate (λ_t) for each GMU (i) and TNWR as a whole:

$$\lambda_{i,t} = \frac{N_{tot,t+1,i}}{N_{tot,t,i}} \tag{3.7}$$

$$\lambda_{tot_t} = \frac{N_{tot,t+1}}{N_{tot,t}} \tag{3.8}$$

Where we added a small quantity (0.001) to the denominator to avoid dividing by zero when abundance in a GMU was small (<5). We also calculated recruitment rate to determine the total amount of calves recruited into the next age class at the end of the year:

$$rec_t = f_t \times \phi_{ca_t} \tag{3.9}$$

3.3.4 Model Implementation and Priors

We estimated abundance and demographic rates from 1997–2020 despite the availability of counts prior to 1997 because usable telemetry data began in 1997. Without demographic rate availability, we did not believe the IPM could provide reliable parameter estimates, and thus did not include count data prior to 1997.

To accommodate using process variance for sensitivity analysis (see Section 3.3.5), we separated sampling and process variance by implementing random effects (Burnham and White, 2002) for annual vital rate estimates. Annual vital rate estimates (say, θ_t) were thus modeled as:

$$\theta_t \sim Normal(\mu, \tau) \tag{3.10}$$

The mean (μ) from Eq. 3.10 was set as a draw from a hyperprior unique to each vital rate. We used non-informative $Uniform(0, 1)$ hyperpriors for calf survival (ϕ_{ca}) and twin-

ning rate (γ) global means, as these are the most variable vital rates within and between large herbivore populations and thus the least predictable (Gaillard et al., 2000). We used informative hyperpriors for the more consistent vital rates, cow survival (ϕ_{cw}) and parturition (α) (Gaillard et al., 2000). We derived the $Beta(30, 2)$ hyperprior for cow survival by evaluating various forms of the beta distribution until we identified a form with good fit for high (>90%) adult survival rates typical of moose (Franzmann and Schwartz, 1998). We derived the $Beta(33.8, 7.75)$ hyperprior for parturition (α) by fitting a beta distribution to long-term parturition means from other long-term moose studies (Appendix Table 5.7) using the fitdistr() function in the package "MASS" (Venables and Ripley, 2002). We set variance (τ) hyperpriors from Eq. 3.10 to non-informative $Uniform(0, 5)$ distributions for adult survival, and parturition and twinning rates (Schaub and Kery, 2021). We widened the calf survival hyperprior for τ to $Uniform(0, 8)$ to accommodate higher-than-expected variance. For detection probabilities, we assigned a non-informative $Uniform(0, 1)$ prior for $p_{calfdetection}$, but deterministically equated p_{count} (Eq. 3.4) to 0.84 based on sightability estimates (Aderman et al., 2019).

Bayesian posterior distributions were sampled from Markov chain Monte Carlo (MCMC) algorithms. Three independent MCMC chains were used with 130,000 iterations, using 10,000 for adaptation, discarding the first 50,000 as burn-in, and thinning each chain by 4 for a total posterior sample size of 60,000. Model convergence was determined by examining traceplots for sufficient mixing, and by ensuring Gelman-Rubin convergence diagnostics, $\hat{R}$, (Brooks and Gelman, 1998) were below 1.1 (Gelman and Hill, 2006). We conducted MCMC simulations in JAGS (Plummer, 2012) accessed using program R version 4.0.5 (R Core Team, 2021) utilizing the jagsUI package (Kellner, 2019).

3.3.5 Sensitivity and Life Table Response Experiments Analysis

We used tLTRE analysis (Koons et al., 2016, 2017) to measure the contribution of variability in each vital rate θ_i (the complement to θ_i is all other vital rates θ_j), including components of population structure, to the temporal variance of realized λ_t:

$$\text{contribution}_{\theta_i}^{var(\lambda_t)} \approx \sum_j \text{cov}(\theta_{i,t}, \theta_{j,t}) \frac{\partial \lambda_t}{\partial \theta_{i,t}} \frac{\partial \lambda_t}{\partial \theta_{j,t}} \bigg|_{\hat{\theta}} \tag{3.11}$$

The resulting contributions measure how strongly fluctuations in λ have been driven by the direct and indirect effects of each vital rate and population structure component (Koons et al., 2016, 2017). The formulization of λ_{t+1} we used for tLTRE was a combination of Eqs. 3.1 and 3.2:

$$\lambda_t = \frac{n2_t * 0.5 * ((\alpha_{t+1} * (\gamma_{t+1} * 2)) + (\alpha_{t+1} * (1 - \gamma_{t+1}))) * \phi_{ca,t+1}) + (\phi_{ad,t+1} * (n1_t + n2_t))}{(n1_t + n2_t)} \tag{3.12}$$

A strength of the formulization of λ_t from tLTRE (eq. 3.12) is that it allows for the use of first derivatives of the λ_t equation with respect to any parameter θ_i, to calculate sensitivities for each θ_i. This is in contrast with more traditional matrix analysis that requires combining reproductive and survival terms to simplified measures of fecundity or recruitment (e.g. combining parturition and twinning into a fecundity term). To show the strength of tLTRE analysis for this study, we compared sensitivities and contributions calculated using tLTRE analysis to sensitivities calculated using traditional two-stage population matrices (see Neubert and Caswell (2000)). There was no direct comparison to our formulization of λ_t (Eq. 3.12), so we created two analogous matrices: (1) a pre-birth pulse model

$$\begin{bmatrix} 0 & rec \\ \phi_{cw} & \phi_{cw} \end{bmatrix} \tag{3.13}$$

where we substituted what should be ϕ_{juv} in the bottom left with ϕ_{cw} because we did not separate juvenile from adult survival, and combined parturition, twinning, and calf survival into a recruitment term (*rec*) (Eq. 3.9); and (2) a post-birth pulse model

$$\begin{bmatrix} 0 & f \\ \phi_{ca} & \phi_{cw} \end{bmatrix} \tag{3.14}$$

where we combined parturition and twinning into a fecundity term (f) (Eq. 3.3). We calculated sensitivities for each component of both matrices by multiplying the complex conjugate of the left eigenvector by the transposed right eigenvector (Caswell, 2000) in R (R Core Team, 2021). For both tLTRE and matrix analyses, we calculated sensitivities for each θ_i estimate from each MCMC draw. For vital rates we were able to include as random effects (adult and calf survival, parturition, and twinning) in the IPM, we used estimates of μ_{θ_i} (Eq. 3.10) as it allowed us to use only process variance in sensitivity analysis (Burnham and White, 2002). We summarized sensitivities and contributions using means and 95% Bayesian Credible Intervals (BCI's) of resulting posterior distributions.

3.4 Results

MCMC chains converged such that traceplots appeared sufficiently mixed, and $\hat{R}$ values remained <1.1. The moose population increased in every GMU over the study time period (1997-2020), and realized population growth rate (λ_t) was >1 for 78 of 92 total study years (Figure 3.4). Population growth rates were variable between GMU's, however, with both sub-GMU's in GMU 18 exhibiting overall higher growth rates than those in GMU 17 (Figure 3.4). Populations began expanding at different times between GMUs, as well, where populations were already increasing at the beginning of the study for both 17A and 17C, but started later in 18: roughly 2004 in 18G, and 2010 in 18KA (Figure 3.4). The moose population across TNWR increased steadily over time, and annual growth rate was > 1 for 18 out of 23 total study years (Figure 3.5a). Population structure varied considerably

between years and did not reach an equilibrium, with annual proportions of calves varying between 0.5 and 31.8% (Figure 3.5b), and vice versa for proportions of adults (Figure 3.5c).

Moose vital rates were variable over time, though some varied more than others (Figure 3.6). Cow survival (ϕ_{cw}) varied the least and averaged 99% overall, while reproductive parameters parturition (α) and twinning (γ) varied moderately and similarly, averaging 61% and 66% overall, respectively. Calf survival (ϕ_{ca}) varied the most and averaged 46% overall (Table 3.1). Fecundity averaged 0.76 calves per cow, and recruitment averaged 0.31 calves per cow.

Sensitivity analysis using matrices and tLTRE analysis indicated that, all else being equal, adult survival would have the greatest potential to affect realized population growth over one year, no matter what composition of reproduction (*rec* or f) adult survival was compared to (Table 3.2). Vital rates did not vary equally over time (Table 3.1), however, and when we took estimated retrospective process covariances among demographic parameters into account (i.e. contributions), we found that fluctuations in calf survival contributed most (~84%) to temporal variation in realized population growth rates. Parturition (5.6%) and adult population proportion (5.6%) contributed moderately toward growth rate temporal variance, followed by twinning (3.4%), and cow survival (1.3%) and calf population proportion (0%) (Figure 3.7 & Table 3.2). Calf population proportion and adult survival sensitivities were mathematically constrained close to 0 and 1 (Table 3.2), respectively, due to their respective partial derivatives within Eq. 3.12.

Importantly, there were many vital rates we could not calculate sensitivities for using matrix models of the TNWR moose population (see dashes in Table 3.2) due to the limitations of the two-stage population matrix model most analogous to the tLTRE analysis.

3.5 Discussion

The moose population in TNWR increased across all four GMUs from 1997–2020, though variance existed and realized population growth rate (λ_t) was not consistently > 1 (Figure 3.4). The population exhibited demographic rates consistent with other ungulate (Gaillard et al., 2000) and Alaska moose populations (Franzmann and Schwartz, 1998; Boertje et al., 2007), though average twinning rate was high, and average parturition was low relative to other studies (Figure 3.6) (Franzmann and Schwartz, 1998; Gaillard et al., 2000). Our results upheld the demographic buffering hypothesis (DBH) (Pfister, 1998) in that the demographic rate with the highest sensitivity, adult survival, (see Table 3.2) had the lowest variability (see Table 3.1). Moreover, that adult survival had the highest sensitivity but lowest variability, and that reproductive terms had lower sensitivities but the highest variability is consistent with the DBH for long-lived animals (Gaillard et al., 2000; Gaillard and Yoccoz, 2003). This indicates that natural selection selects for adults with high resistance to mortality and low expenditure towards offspring production (Gaillard and Yoccoz, 2003). Our tLTRE analysis suggests that an outcome of variability reduction in high sensitivity vital rates is that the vital rate with the highest variability - in our case calf survival - ultimately has the biggest actual impact on variance of λ (Figure 3.7). This has significant implications for the management and conservation of species, where efforts might focus on maintaining high sensitivity vital rates that ultimately won't affect λ. Essentially, natural selection already maintains high sensitivity vital rates by - in this case - selecting for more robust adults, and more vulnerable calves. So by focusing conservation efforts away from highest sensitivity vital rates and towards higher variability, lower sensitivity vital rates like calf survival, conservationists and managers might have more success conserving populations. This statement may only be true when adult survival is free of high predation pressure, direct anthropogenic forces, or other factors that might suppress adult survival. Given how nascent tLTRE analysis is, more studies should be conducted to find patterns between variability, sensitivity, contributions and external factors among long-lived herbivores.

That our results are so in line with other long-lived ungulates indicates that this moose population, though on the edge of its current range, is not in peripheral habitat. More specifically, high adult survival rate compared to other moose populations (Gaillard et al., 2000; Franzmann and Schwartz, 1998; Oates et al., 2021), low adult survival variability similar to other healthy populations (Gaillard et al., 2000), and that calf survival is the most variable vital rate (Eberhardt, 2002) all indicate this population is below carrying capacity, and nutritionally healthy. Based on geography alone, this moose population could be considered to live at the edge of its niche, but our study suggests the population is, at least overall, well within its physiological limits. This is especially true when comparing this population to one along the species' southern periphery, where low relative rates and high variance in adult survival are thought to result from high density dependence and inhabiting sub-optimal environmental conditions (Oates et al., 2021).

Contrary to most previous studies, we found that parturition process variance was higher than that of twinning (Table 3.1). Gaillard et al. (2000) reported the opposite for polytocous ungulates in general, and moose specifically (see also (Boer, 1992)). Given gestation is, relative to lactation, not very physiologically intensive, Gaillard et al. (2000) argued that parturition probability for a nutritionally sufficient population should more or less be constant across a variety of environmental conditions. A possible explanation for our anomalous results is that calf detection during the first weeks of parturition is low and subject to changing conditions (ie, early leaf-out, bad flying conditions). Lower variance for twinning may be due to there being twice as many calves during an observation event, and therefore higher likelihood of returning to check for more calves. Partitioning calf detection by year could account for calves not detected in low-detection years, and stabilize parturition variance.

To our knowledge, this study is the first to implement transient contribution analysis for an ungulate, and we found that variance in calf survival contributed the most to variance in population growth rate (Figure 3.7). This indicates that population growth rate was most limited by calf survival, and thus the factors that caused variation in calf survival; understanding what those factors are in ungulates can elucidate what caused variability in population growth rates. Outside of predation, which can dominate calf survival dynamics when strongly present (Ballard et al., 1991; Bertram and Vivion, 2002; Keech et al., 2011), annual calf survival is often determined by body mass by the end of the growing season, which, in turn, is determined by forage productivity (Couturier et al., 2009; McArt et al., 2009; Hurley et al., 2014), forage diversity (Felton et al., 2020, 2021), and the length of the growing season (Hurley et al., 2014; Loe et al., 2021). Since predation pressure likely was low over the study time period (Aderman, 2014), the results from this study suggest that population growth rate was limited by growing season productivity and its effects on calf survival. Moreover, that calf survival was most variable in this population might indicate it is below carrying capacity; Eberhardt (2002) hypothesized a paradigm of chronological vital rate change as long-lived vertebrate populations reach carrying capacity, where calf survival is the most vulnerable vital rate, followed by fecundity, then by adult survival. Contribution of vital rates by year is needed (e.g. Koons et al., 2017; Taylor et al., 2018; Schaub and Kery, 2021), however, to confirm whether there is a change in vital rate contribution as this population increased.

Our results can help us answer the question of why moose populations have only recently increased in TNWR. It seems clear that current conditions are amenable to a healthy moose population, but southwest Alaska's climate and ecology have changed substantially in recent decades (Walsh and Brettschneider, 2019; Potter and Alexander, 2020; Frost et al., 2021; Macander et al., 2022). It is possible, then, that TNWR had sub-optimal conditions that only sustained low-density populations prior to the sudden increase. The speed at which

the population grew, suggests, then, a mismatch between their actual and their potential geographic distribution. This mismatch, coined range boundary disequilibrium, can reflect differences in dispersal, life history, recolonization history, or stochasticity (Sexton et al., 2009). Given data limitations on many environmental and ecological conditions at the time, we can only speculate as to the reasons behind the disequilibrium, but it is difficult to ignore the irruption of the local Mulchatna caribou herd (MCH) in the 1990s (Valkenburg et al., 2003) that could have diverted hunting pressure away from low-density moose (Aderman, 2014). As we did find adult survival to have the highest potential impact on population growth rate, hunting pressure on cows could have suppressed population growth until that hunting pressure was released. Population growth after the MCH crash could be attributed to work between local hunters and TNWR managers that led to various hunting moratoriums that could have helped establish high-density moose populations (Aderman, 2014). Therefore, we argue the most likely causes are a combination between improving habitat due to climate change, and a dispersal barrier caused by human hunting pressure.

Additionally, the later population increases in GMUs 18G and 18KA than in 17A and 17C (Figure 3.4) suggest immigration from the east, as hypothesized by Aderman (2014), which likely supplemented growth happening within TNWR after initial population increase began. Though a strength of IPMs is the ability to estimate unobserved parameters like immigration (Abadi et al., 2010), we chose not to after difficulties with convergence; likely, the large temporal gaps between counts could not accommodate an unobserved parameter. The pattern of later western population increases also indicates the colonization of moose in western TNWR. Early reports of moose in the area only noted moose in the Togiak Valley (Abercrombie et al., 1900), but did not explicitly state that moose did not inhabit the further west Ahklun mountains. These reports, as well as consistently zero moose counts implemented by TNWR before the mid-2000s in 18G and 18KA (Figure 3.4) suggest colonizing moose populations in the Goodnews, Kanektok, and Arolik drainages.

We hope this study can pave the way for greater insight in environmental and demographic drivers, and life history of long-lived ungulates and, more generally, long-lived vertebrates. tLTREs, and the IPMs that usually accompany them, are valuable new tools for ecologists (Koons et al., 2016, 2017); conducting more tLTREs and IPMs on ungulate populations in a variety of habitats and demographic conditions will broaden our understanding of which population parameters actually operate on growth rate in time-varying environments, and therefore inform effective conservation measures (see Zipkin and Saunders (2018) for more discussion). Our analysis additionally demonstrates the usefulness of calculating sensitivity using the formulization of λ_t (Eq. 3.12) used in Koons et al. (2016), compared to traditional matrix calculations. Though some parameters were constrained, we were able to decompose recruitment and fecundity to understand the role of all the parameters we were able to estimate (Table 3.2). Building upon overall contributions, and extending tLTRE analysis to successive time steps could yield even more detailed knowledge for how demographic parameters affect population growth rate, including whether contributions change as the population grows.

3.6 Acknowledgements

We thank the many pilots and observers who, over four decades, collected data for this project. We thank C. Mulder, K. Tape, S. Swanson, and D. Arnold for helpful comments on drafts of the manuscript. This work was funded through the US Fish and Wildlife Service, the Luick Memorial Travel Fund, the Calvin J. Lensink Fellowship, and two Teaching Assistantships from the UAF Department of Biology. We acknowledge that this work took place on ancestral homelands of Yup'ik and lower Tanana Dené lands, and are grateful for their stewardship of these lands since time immemorial. Any use of trade, firm, or product names is for descriptive purposes only and does not imply endorsement by the U.S. Government. The findings and conclusions in this article are those of the author(s) and do

not necessarily represent the views of the U.S. Fish and Wildlife Service.

3.7 References

Abadi, F., O. Gimenez, R. Arlettaz, and M. Schaub (2010). An assessment of integrated population models: bias, accuracy, and violation of the assumption of independence. *Ecology 91*, 7–14.

Abadi, F., O. Gimenez, B. Ullrich, R. Arlettaz, and M. Schaub (2010). Estimation of immigration rate using integrated population models. *Journal of Applied Ecology 47*(2), 393–400.

Abercrombie, W. R., E. F. Glenn, O. O. Howard, I. Petroff, P. H. Ray, W. P. Richardson, and E. H. Wells (1900). *Compilation of Narratives of Explorations in Alaska.* Number 1023. US Government Printing Office.

Aderman, A. (2014). Monitoring moose demographics at Togiak National Wildlife Refuge, southwestern Alaska, 1998-2013. *Togiak National Wildlife Refuge, Dillingham, Alaska.*, 1–25.

Aderman, A., N. Barten, and M. Higham (2019). Estimation of moose abundance using the geospatial population estimator combined with a sightability model on Togiak NWR; final project report. *Western Alaska Landscape Conservation Cooperative Project*, 1–16.

Alaska Climate Research Center (2022a). Precipitation normals. Available at https://akclimate.org/data/precipitation-normals/.

Alaska Climate Research Center (2022b). Temperature normals. Available at https://akclimate.org/data/air-temperature-normals/.

Ballard, W. B., J. S. Whitman, and D. J. Reed (1991). Population dynamics of moose in south-central Alaska. *Wildlife Monographs*, 3–49.

Bertram, M. R. and M. T. Vivion (2002). Moose mortality in eastern interior Alaska. *The Journal of Wildlife Management 66*, 747–756.

Boer, A. H. (1992). Fecundity of North American moose (*Alces alces*): a review. *Alces: A Journal Devoted to the Biology and Management of Moose*, 1–10.

Boertje, R. D., K. A. Kellie, C. T. Seaton, M. A. Keech, D. D. Young, B. W. Dale, L. G. Adams, and A. R. Aderman (2007). Ranking Alaska moose nutrition: Signals to begin liberal antlerless harvests. *Journal of Wildlife Management 71*, 1494–1506.

Brooks, S., R. King, and B. Morgan (2004). A Bayesian approach to combining animal abundance and demographic data. *Animal biodiversity and conservation 27*(1), 515–529.

Brooks, S. P. and A. Gelman (1998). General methods for monitoring convergence of iterative simulations. *Journal of Computational and Graphical Statistics 7*, 434–455.

Burnham, K. P. and G. C. White (2002). Evaluation of some random effects methodology applicable to bird ringing data. *Journal of Applied Statistics 29*, 245–264.

Caswell, H. (1989). Analysis of life table response experiments I. Decomposition of effects on population growth rate. *Ecological Modelling 46*, 221–237.

Caswell, H. (2000). *Matrix population models*, Volume 1. Sinauer Sunderland.

Couturier, S., S. D. Côté, R. D. Otto, R. B. Weladji, and J. Huot (2009). Variation in calf body mass in migratory caribou: the role of habitat, climate, and movements. *Journal of Mammalogy 90*(2), 442–452.

Eberhardt, L. (2002). A paradigm for population analysis of long-lived vertebrates. *Ecology 83*(10), 2841–2854.

Felton, A. M., E. Holmström, J. Malmsten, A. Felton, J. P. Cromsigt, L. Edenius, G. Ericsson, F. Widemo, and H. K. Wam (2020). Varied diets, including broadleaved forage, are important for a large herbivore species inhabiting highly modified landscapes. *Scientific Reports 10*.

Felton, A. M., H. K. Wam, A. Felton, S. J. Simpson, C. Stolter, P. O. Hedwall, J. Malmsten, T. Eriksson, M. Tigabo, and D. Raubenheimer (2021). Macronutrient balancing in free-ranging populations of moose. *Ecology and Evolution 11*, 11223–11240.

Franzmann, A. W. and C. C. Schwartz (1998). *Ecology and Management of the North American Moose* (1 ed.). Wildlife Management Institute.

Frost, G. V., U. S. Bhatt, M. J. Macander, A. S. Hendricks, and M. T. Jorgenson (2021). Is Alaska's Yukon–Kuskokwim Delta greening or browning? Resolving mixed signals of tundra vegetation dynamics and drivers in the maritime Arctic. *Earth Interactions 25*, 76–93.

Gaillard, J.-M., M. Festa-Bianchet, N. G. Yoccoz, A. Loison, and C. Toigo (2000). Temporal variation in fitness components and population dynamics of large herbivores. *Annual Review of Ecology and Systematics 31*, 367–393.

Gaillard, J.-M. and N. G. Yoccoz (2003). Temporal variation in survival of mammals: a case of environmental canalization? *Ecology 84*, 3294–3306.

Gelman, A. and J. Hill (2006). *Data analysis using regression and multilevel/hierarchical models*. Cambridge University Press.

Gillespie, J. H. (1977). Natural selection for variances in offspring numbers: a new evolutionary principle. *The American Naturalist 111*(981), 1010–1014.

Hurley, M. A., M. Hebblewhite, J.-M. Gaillard, S. Dray, K. A. Taylor, W. K. Smith, P. Zager, and C. Bonenfant (2014). Functional analysis of normalized difference vegetation index curves reveals overwinter mule deer survival is driven by both spring and autumn phenology. *Philosophical Transactions of the Royal Society B: Biological Sciences 369*, 20130196.

Keech, M. A., M. S. Lindberg, R. D. Boertje, P. Valkenburg, B. D. Taras, T. A. Boudreau, and K. B. Beckmen (2011). Effects of predator treatments, individual traits, and environment on moose survival in Alaska. *Journal of Wildlife Management 75*, 1361–1380.

Kellner, K. (2019). jagsui: A wrapper around 'rjags' to streamline 'jags' analyses. R package version 1.5.1.

Koons, D. N., T. W. Arnold, and M. Schaub (2017). Understanding the demographic drivers of realized population growth rates. *Ecological Applications 27*(7), 2102–2115.

Koons, D. N., D. T. Iles, M. Schaub, and H. Caswell (2016). A life-history perspective on the demographic drivers of structured population dynamics in changing environments. *Ecology Letters 19*, 1023–1031.

Langenau Jr, E. and J. Lerg (1976). The effects of winter nutritional stress on maternal and neonatal behavior in penned white-tailed deer. *Applied Animal Ethology 2*(3), 207–223.

Loe, L. E., G. E. Liston, G. Pigeon, K. Barker, N. Horvitz, A. Stien, M. Forchhammer, W. M. Getz, R. J. Irvine, and A. Lee (2021). The neglected season: Warmer autumns counteract harsher winters and promote population growth in arctic reindeer. *Global Change Biology 27*(5), 993–1002.

Macander, M. J., P. R. Nelson, T. Nawrocki, G. V. Frost, K. Orndahl, E. C. Palm, A. F. Wells, and S. J. Goetz (2022). Time-series maps reveal widespread change in plant functional type cover across arctic and boreal Alaska and Yukon. *Environmental Research Letters 17*(5), 054042.

Maunder, M. N. and A. E. Punt (2013). A review of integrated analysis in fisheries stock assessment. *Fisheries Research 142*, 61–74.

McArt, S. H., D. E. Spalinger, W. B. Collins, E. R. Schoen, T. Stevenson, and M. Bucho (2009). Summer dietary nitrogen availability as a potential bottom-up constraint on moose in south-central Alaska. *Ecology 90*, 1400–1411.

Neubert, M. G. and H. Caswell (2000). Density-dependent vital rates and their population dynamic consequences. *Journal of Mathematical Biology 41*(2), 103–121.

Oates, B. A., K. L. Monteith, J. R. Goheen, J. A. Merkle, G. L. Fralick, and M. J. Kauffman (2021). Detecting resource limitation in a large herbivore population is enhanced with measures of nutritional condition. *Frontiers in Ecology and Evolution 8*.

Pfister, C. A. (1998). Patterns of variance in stage-structured populations: evolutionary predictions and ecological implications. *Proceedings of the National Academy of Sciences 95*(1), 213–218.

Plummer, M. (2012). JAGS version 3.4.0 user manual.

Potter, C. and O. Alexander (2020). Changes in vegetation phenology and productivity in Alaska over the past two decades. *Remote Sensing 12*, 1546.

R Core Team (2021). R: A language and environment for statistical computing.

Rotella, J. J., W. A. Link, T. Chambert, G. E. Stauffer, and R. A. Garrott (2012). Evaluating the demographic buffering hypothesis with vital rates estimated for Weddell seals from 30 years of mark–recapture data. *Journal of Animal Ecology 81*(1), 162–173.

Schaub, M. and F. Abadi (2011). Integrated population models: a novel analysis framework for deeper insights into population dynamics. *Journal of Ornithology 152*, 227–237.

Schaub, M., O. Gimenez, A. Sierro, and R. Arlettaz (2007). Use of integrated modeling to enhance estimates of population dynamics obtained from limited data. *Conservation Biology 21*(4), 945–955.

Schaub, M. and M. Kery (2021). *Integrated population models: theory and ecological applications with R and JAGS.* Academic Press.

Sexton, J. P., P. J. McIntyre, A. L. Angert, and K. J. Rice (2009). Evolution and ecology of species range limits. *Annual Review of Ecology, Evolution and Systematics 40*(1), 415–436.

Sher, A. (2022). *An introduction to conservation biology.* Oxford University Press.

Taylor, L. U., B. K. Woodworth, B. K. Sandercock, and N. T. Wheelwright (2018). Demographic drivers of collapse in an island population of tree swallows. *The Condor: Ornithological Applications 120*(4), 828–841.

Tuljapurkar, S. (1990). *Population dynamics in variable environments*, Volume 85. Springer Science & Business Media.

Valkenburg, P., R. A. Sellers, R. C. Squibb, J. D. Woolington, A. R. Aderman, and B. W. Dale (2003). Population dynamics of caribou herds in southwestern Alaska. *Rangifer 23*(5), 131–142.

Venables, W. N. and B. D. Ripley (2002). *Modern Applied Statistics with S* (Fourth ed.). Springer. ISBN 0-387-95457-0.

Viereck, L. (1979). Characteristics of treeline plant communities in Alaska. *Holarctic Ecology 2*, 228–238.

Walsh, J. E. and B. Brettschneider (2019). Attribution of recent warming in Alaska. *Polar Science 21*, 101–109.

Wisdom, M. J., L. S. Mills, and D. F. Doak (2000). Life stage simulation analysis: estimating vital-rate effects on population growth for conservation. *Ecology 81*(3), 628–641.

Zipkin, E. F. and S. P. Saunders (2018). Synthesizing multiple data types for biological conservation using integrated population models. *Biological Conservation 217*, 240–250.

3.8 Figures

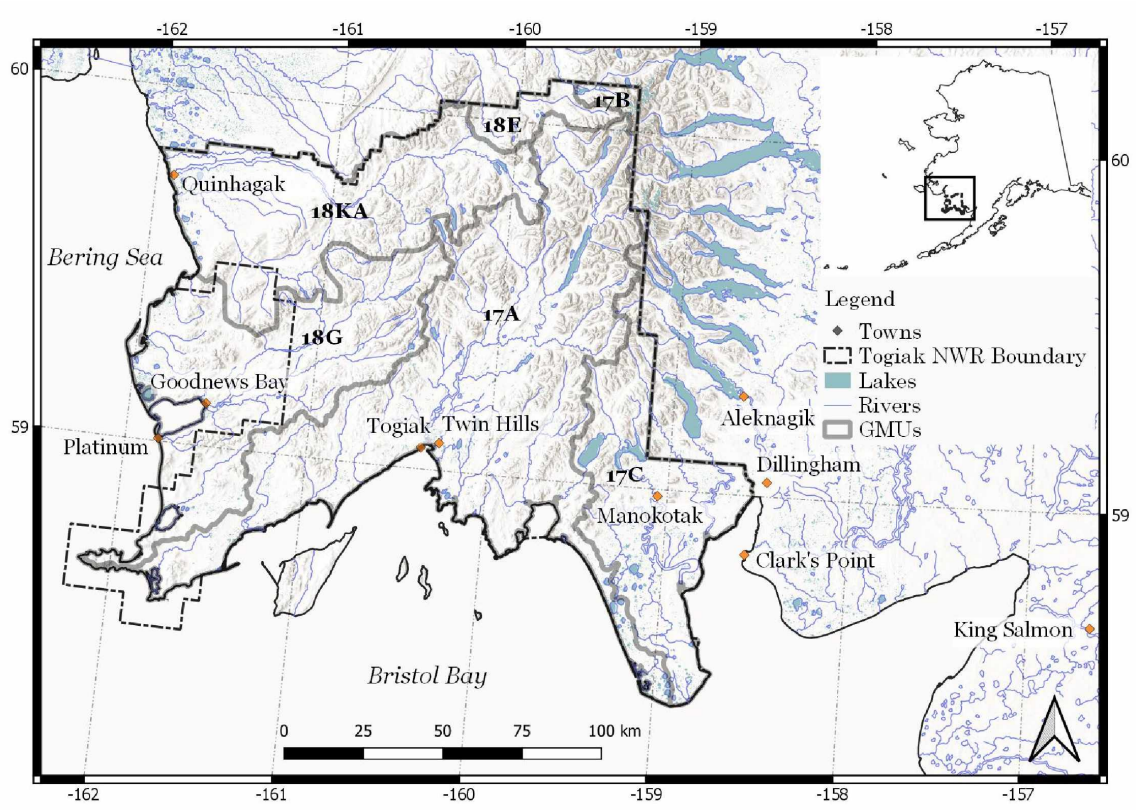

Figure 3.1: Togiak National Wildlife Refuge (TNWR) boundary and Game Management Units (GMUs) in which radio telemetry and population counts were conducted.

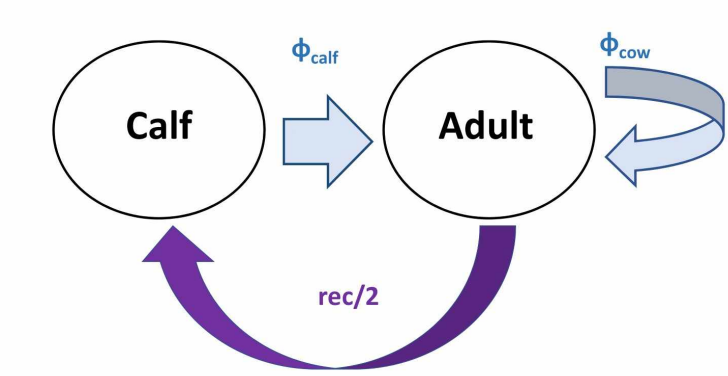

Figure 3.2: Simplified life stages and transition probabilities used in the population model of the IPM. ϕ represents survival, and *rec* represents recruitment, a function of parturition, twinning, and calf survival probabilities.

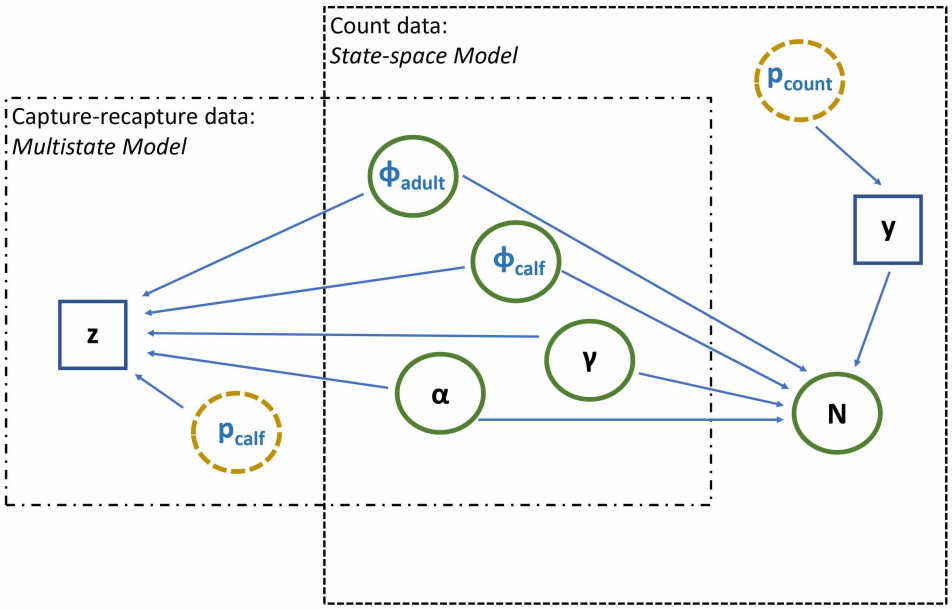

Figure 3.3: Directed acyclic graph representing the structure of the models within the IPM. Estimated parameters are shown in circles, where dashed circles are parameters from the observation process, and bolded circles are parameters from the state process, and data are shown in rectangles. Arrows represent dependencies between nodes. Node notations: y is count data, z is telemetry data, ϕ is survival, α is parturition, γ is twinning, and p is detection probability.

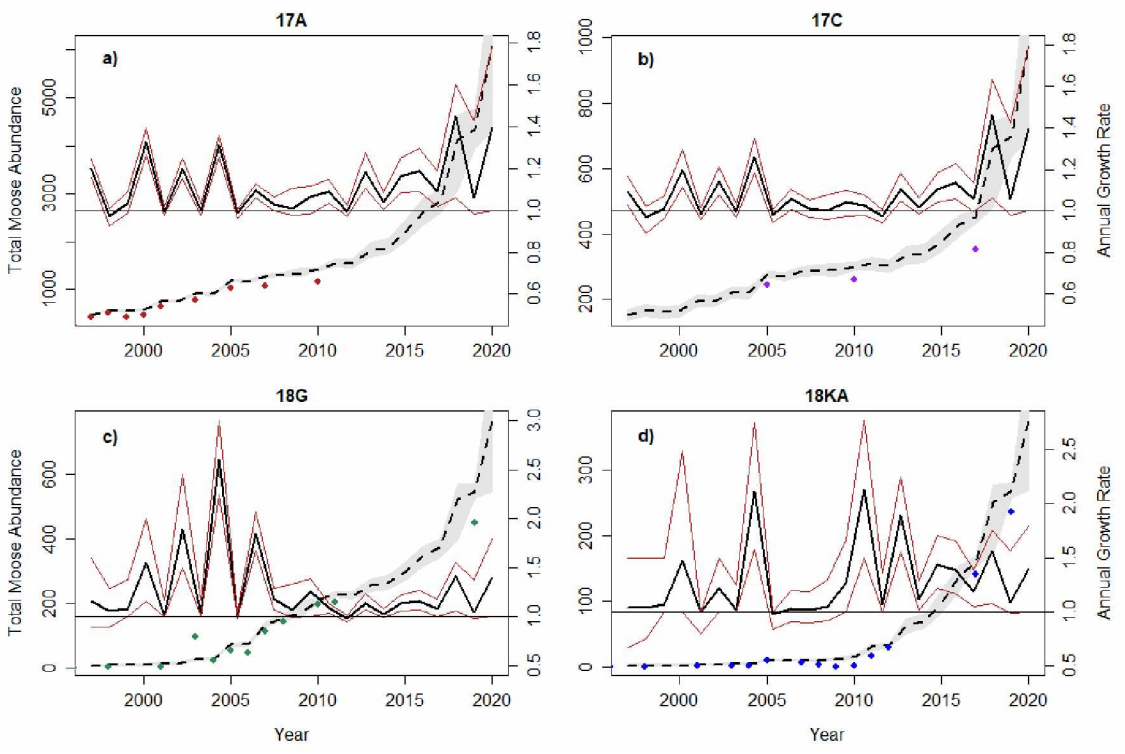

Figure 3.4: Population trajectories and annual growth rate for every Game Management Unit (GMU) included in the study: a) 17A, b) 17C, c) 18-Goodnews (18G), and d) 18-Kanektok-Arolik (18KA). Solid black lines indicate annual population growth rate means (λ_t), red lines indicate upper and lower 95% Bayesian Credible Intervals (BCI) for growth rate. Dashed lines indicate estimated annual abundance, grey shading represents 95% BCI's for abundance, and colored dots represent raw count data. Note different y-axes for each graph.

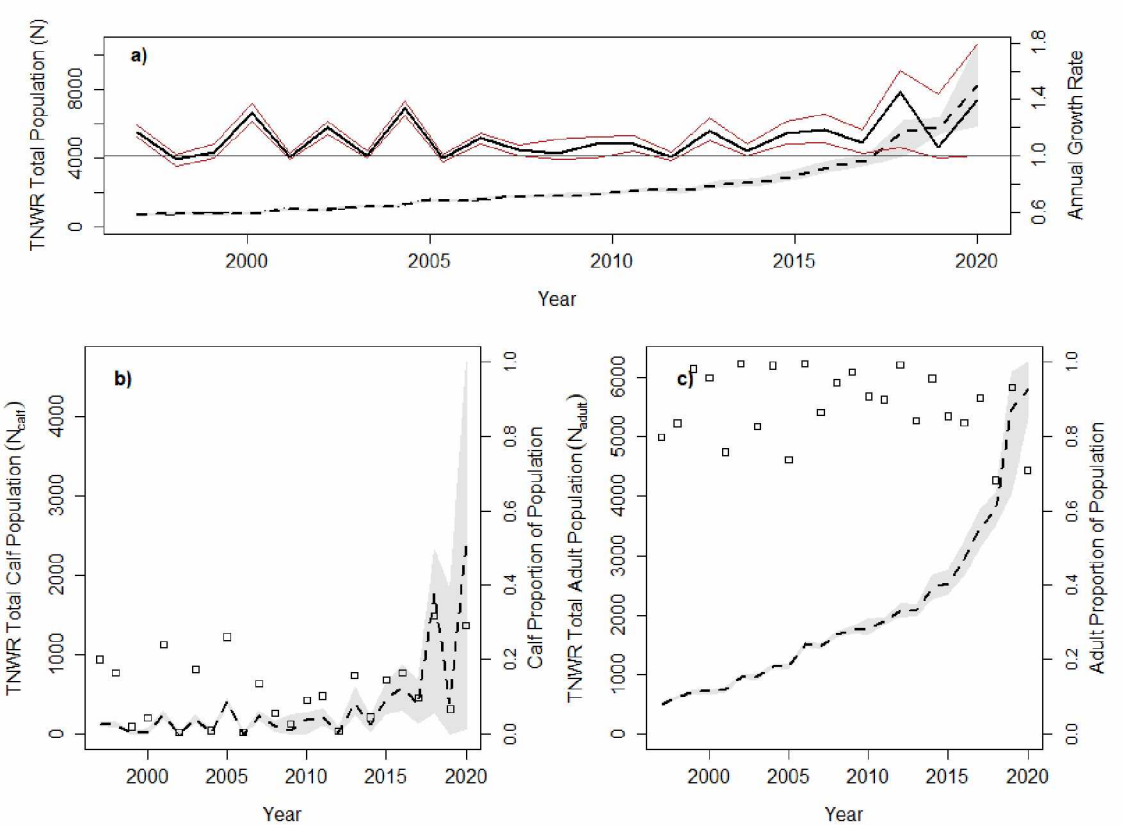

Figure 3.5: Annual population structure for Togiak National Wildlife Refuge (TNWR), calculated as the sum of moose from each Game Management Unit (GMU). a) shows TNWR annual population growth rate and estimated abundance (N), b) shows TNWR annual estimated calf abundance (N_{calf}) and annual proportion of the population that was a calf (squares), and c) shows TNWR annual estimated adult abundance (N_{adult}) and the annual proportion of the population that were adults (squares).

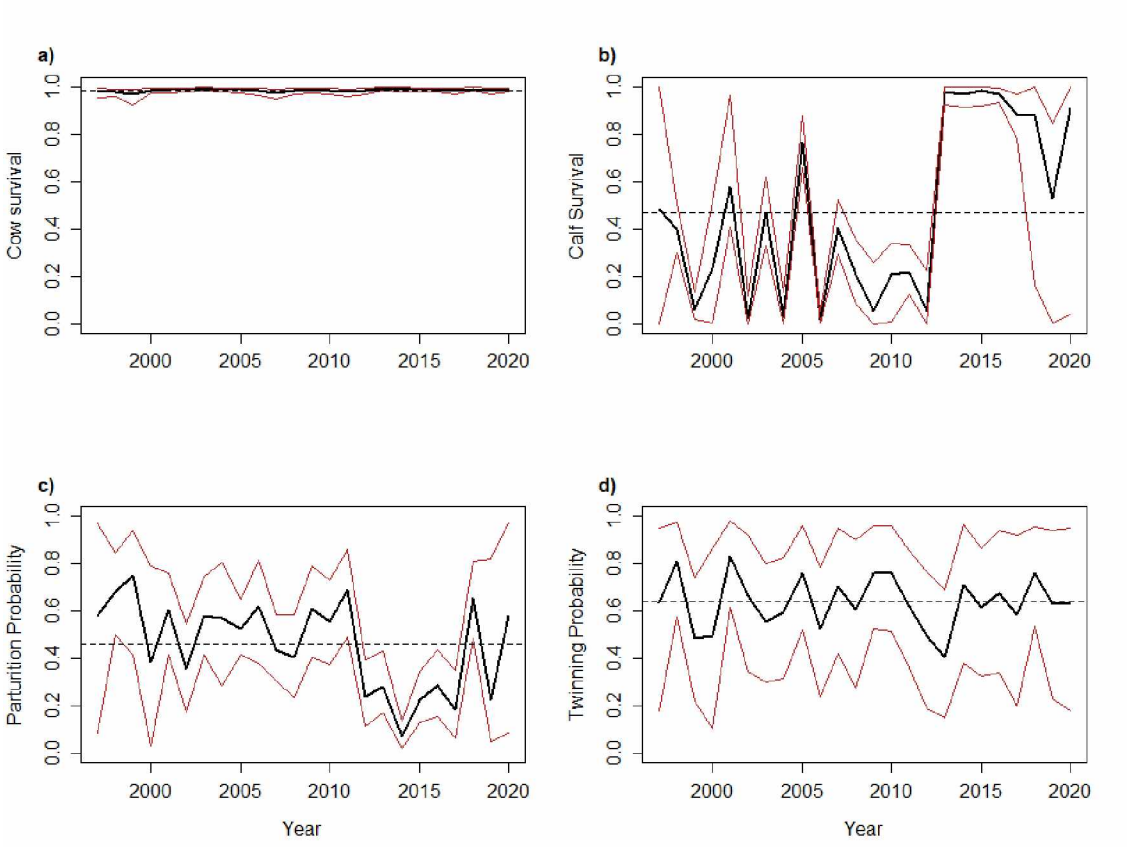

Figure 3.6: Annual estimates of demographic parameters, where each year constituted an independent draw from a Normal distribution (i.e. a random effect of year), including a) cow survival probability, b) calf survival probability, c) parturition probability, and d) twinning probability. Solid black lines indicate posterior annual means, dashed lines represent overall means, and red lines indicate upper and lower 95% Bayesian Credible Intervals.

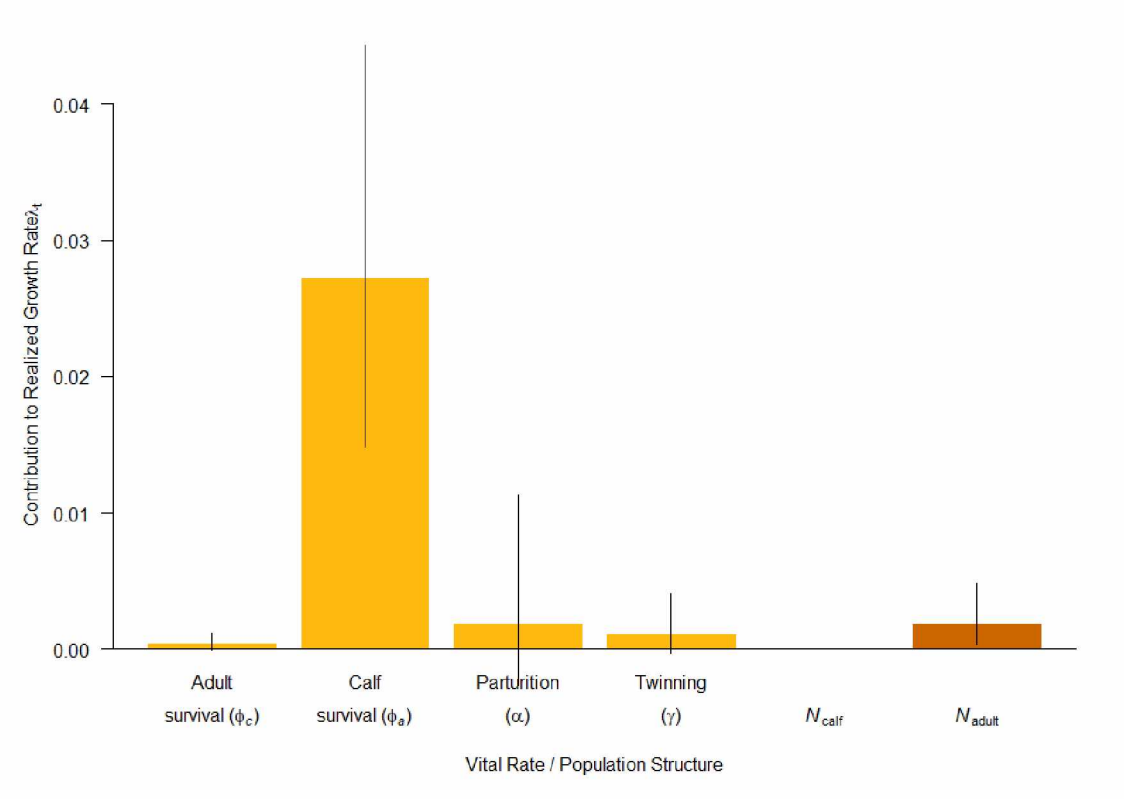

Figure 3.7: Contributions from each vital rate and population structure to annual realized growth rate (λ_t). Yellow bars indicate vital rates, orange bars indicate population structure, and lines represent 95% Bayesian Credible Interval (BCI) of the posterior distribution.

3.9 Tables

Table 3.1: Posterior mean (μ) and 95% Bayesian Credible Intervals (BCI) of Normal distribution means and standard deviations (σ) from which all demographic rates were sampled (Eq. 3.10).

demographic rate	mean μ	95% BCI	mean σ	95% BCI
ϕ_{cw}	0.99	0.98 - 0.99	0.56	0.08 - 1.05
ϕ_{ca}	0.46	0.17 - 0.78	3.62	2.33 - 5.7
α	0.61	0.49 - 0.74	1.40	0.89 - 2.2
γ	0.66	0.53 - 0.8	0.97	0.24 - 1.94

Table 3.2: Comparison of sensitivities (sens) of demographic parameters as calculated using a pre-birth matrix (Eq. 3.13), a post-birth matrix (Eq. 3.14), and tLTRE analysis, and contributions of demographic parameters to λ_t calculated using tLTRE. (*) indicates a different "lambda" configuration (Eq. 3.12) was used to combine elements of either fecundity (f) or recruitment (rec). Dashes indicate sensitivities that were not possible to calculate given the limitations of calculating sensitivity using matrix models. Symbols and abbreviations for demographic parameters are as described following Eqs. 3.1, 3.2 & 3.3.

parameter	Pre-birth matrix sens	Post-birth matrix sens	tLTRE sens	tLTRE contribution
ϕ_{cw}	0.832 (0.818,0.846)	0.825 (0.776,0.889)	1 (1,1)	0 (0,0.001)
ϕ_{ca}	-	0.501 (0.417,0.612)	0.451 (0.37,0.539)	0.027 (0.016,0.041)
α	-	-	0.342 (0.154,0.542)	0.002 (-0.002,0.009)
γ	-	-	0.126 (0.056,0.205)	0.001 (0,0.003)
f	-	0.295 (0.164,0.412)	0.206 (0.093,0.326)*	0.004 (-0.001,0.011)*
rec	0.664 (0.636,0.692)	-	0.445 (0.443,0.447)*	0.02 (0.012,0.031)*
n1	-	-	0.00 (0.00,0.00)	0.00 (0.00,0.00)
n2	-	-	0.235 (0.104,0.382)	0.002 (0,0.004)

Chapter 4: General Conclusions

Understanding drivers of population dynamics is vital to conservation and management of species. In this thesis, I investigated environmental and demographic drivers of a rapidly expanding moose population to 1) form greater understanding of how stochastic processes affect population dynamics of large herbivores, and 2) elucidate reasons for the sudden colonization of moose in this part of the sub-Arctic. In my second chapter, I correlated environmental conditions to moose population demographic rates using a multistate model, and in my third chapter I examined contributions of demographic rates on population growth rate by employing transient life table response experiments (tLTREs) within an integrated population model (IPM). Together, these two chapters paint a picture of how environmental conditions affect population growth rate via effects on demographics. More specifically, I found that vegetation productivity and winter severity affected calf survival most strongly, and, in turn, variance in calf survival contributed more to variance in population growth than any other demographic rate. These results suggest that vegetation productivity and winter severity affected population growth rate through their effects on calf survival, though I did not directly calculate how variance in environmental conditions contributed to population growth rate. Because both environmental factors I included changed over long time spans due to climate change (see also (Walsh and Brettschneider, 2019; Lader et al., 2020; Frost et al., 2021; Macander et al., 2022)), the results of this thesis indicate that climate change likely played an important role in the rapid moose population increase in southwest Alaska.

The lack of trends of components of climate change over my study time period, however, complicates this narrative; abundance estimates from the IPM in chapter 3 made it clear that this population increased rapidly regardless of environmental conditions. Still, the fact that NDVI and WSI explained variance in calf survival and twinning in chapter 2 could indicate that environmentally limited population growth rate could have occurred before

temperatures started increasing in the region. To synthesize arguments made in chapters 2 and 3, a possible explanation for the discrepancy in the lack of short-term environmental changes and rapid population growth rate is this population experienced range boundary disequilibrium (Sexton et al., 2009) as habitat improved with warming temperatures, but human hunting pressure didn't allow moose dispersal into TNWR to form a sustainable population. It wasn't until the Mulchatna caribou herd (MCH) grew rapidly in the 1980s and 1990s (Valkenburg et al., 2003) that hunting pressure diverted away from moose (Aderman, 2014), and allowed them to flourish in newly suitable habitat.

This explanation follows the hypotheses from Tape et al. (2016) and Aderman (2014) but contradicts Groves et al. (2022), who argued recent moose colonization of the western North American Arctic is unrelated to climate change, and rather a function of high mobility and fluctuation-prone metapopulations. Historical narratives (see (Abercrombie et al., 1900; Kowta, 1963)) support low density moose populations in the Togiak Valley in the late 1800s, and likely before that, but little is known about population fluctuations before the 1950s. Theoretically, then, this latest population increase could be a fluctuation that has happened before, which would support the argument made by Groves et al. (2022). But the fact that moose bones were not found in an archaeological dig in the Togiak Valley (Kowta, 1963) suggests moose rarely, if ever, reached high densities, even when caribou populations were high, as they likely were in the 1860s (Skoog, 1968). Additionally, the abrupt increase of the moose population in the 1990s, known vulnerability to food availability in periphery ranges (Ruprecht et al., 2020; Oates et al., 2021), increases in annual temperatures in the region, and correlations between environmental conditions I found in chapter 2 support a climate change hypothesis modified by human intervention, similar to the hypothesis established by Tape et al. (2016). As such, the consistent lack of any moose counted in 18G and 18KA — the farthest west portions of TNWR — prior to the early 2000s followed by rapid increases (Figure 3.4) could represent novel moose populations in those areas, and thus, a

colonization event. Ultimately, these results have important implications not just for moose across Alaska, but any species whose ranges may be transforming with climate change; while warmer temperatures are altering animal ranges (Chen et al., 2011; Bellard et al., 2012), human activity plays an important role in what area a species can actually inhabit.

The inferences made in this project are principally due to the existence of TNWR's long-term monitoring project; this effort underscores the need to maintain these kinds of projects that span decades of ecological and climatological patterns. The advent of Bayesian statistics since the inception of the project was extremely fortunate, as our models were able to handle the many gaps in data (Schaub et al., 2007) that inherently exist in such a logistically challenging environment. Data collection in TNWR for this project continues to the present day, and data since 2020 (after our study) indicate a shift toward consistently low calf survival (Aderman, unpublished data). This follows the pattern since the mid-2010s of continuous low calf survival east of TNWR — outside of our study area — that has been attributed to higher than normal bear predation on moose calves (Alaska Department of Fish and Game, unpublished data). Though the hypothesis of the chronology of vital rates as a population nears carrying capacity (Eberhardt, 2002) would suggest a decline in calf survival as the first sign of increasing density dependence, record salmon runs in the region in past years (Alaska Department of Fish and Game, unpublished data) could be increasing bear density. In a form of apparent competition, bears emerging from hibernation before salmon run up rivers, and other food sources becoming scarce as bear density increases, bears could be turning towards more risky moose calves for sustenance. Nonetheless, the recent changing dynamics further underscore the need to maintain continuous datasets like this one.

Potentially changing community dynamics in southwest Alaska highlights another strength of this project: the framework of the IPM. The integrated framework allows for additions of many types of data (Schaub and Kery, 2021), including those of other species (see Quéroué

et al. (2021) for an example of a multispecies IPM). The existing moose IPM provides a structure usable for other adjoining moose populations, and ungulate species, as well as integration of other count data types (especially GSPEs (Schmidt et al., 2022)) and other species counts. Given similar data types over the same time period for moose east of TNWR, caribou in the declining Mulchatna and Nushagak Peninsula caribou herds, and spatially explicit salmon escapement estimates, a study of community dynamics in the face of climate change is alluring.

Additionally, the small component of individual heterogeneity I included in chapter 2 does not exhaustively evaluate how individual quality affects population dynamics. Multistate models are a powerful tool as "states" can be translated to many different definitions (Lebreton et al., 2009). For example, the estimation in another study of state transition between "initially a first time breeder", "breeder", and "non-breeder" led to powerful inference about how individual reproductive performance changed as population density increased (Badger et al., 2020). A similar configuration could lead to a deeper understanding about how individual heterogeneity affects population growth in a moose population, especially one that is increasing so quickly. A spatial aspect to this kind of analysis could also incorporate questions regarding life history strategy differences between colonizers (those moose at the western edge of the TNWR range) and those closer to the core of the range (those on the eastern border) that have been shown to drive evolution and faster growth rates of colonizing populations (Szűcs et al., 2017).

Ultimately, this thesis answers important questions about both specific ecological community change in the sub-Arctic, and broader questions about life history strategy of large herbivores. The construction of the multistate and integrated population models are also exciting jumping boards for further analysis that can answer deeper questions about large herbivore population dynamics, life history, and evolution.

4.1 References

Abercrombie, W. R., E. F. Glenn, O. O. Howard, I. Petroff, P. H. Ray, W. P. Richardson, and E. H. Wells (1900). *Compilation of Narratives of Explorations in Alaska.* Number 1023. US Government Printing Office.

Aderman, A. (2014). Monitoring moose demographics at Togiak National Wildlife Refuge, southwestern Alaska, 1998-2013. *Togiak National Wildlife Refuge, Dillingham, Alaska.*, 1–25.

Badger, J. J., W. D. Bowen, C. E. den Heyer, and G. A. Breed (2020). Variation in individual reproductive performance amplified with population size in a long-lived carnivore. *Ecology 101*, e03024.

Bellard, C., C. Bertelsmeier, P. Leadley, W. Thuiller, and F. Courchamp (2012). Impacts of climate change on the future of biodiversity. *Ecology Letters 15*, 365–377.

Chen, I. C., J. K. Hill, R. Ohlemüller, D. B. Roy, and C. D. Thomas (2011). Rapid range shifts of species associated with high levels of climate warming. *Science 333*, 1024–1026.

Eberhardt, L. (2002). A paradigm for population analysis of long-lived vertebrates. *Ecology 83*(10), 2841–2854.

Frost, G. V., U. S. Bhatt, M. J. Macander, A. S. Hendricks, and M. T. Jorgenson (2021). Is Alaska's Yukon–Kuskokwim Delta greening or browning? Resolving mixed signals of tundra vegetation dynamics and drivers in the maritime Arctic. *Earth Interactions 25*, 76–93.

Groves, P., D. H. Mann, and M. L. Kunz (2022). Prehistoric perspectives can help interpret the present: 14,000 years of moose (*Alces alces* l) in the Western Arctic. *Canadian Journal of Zoology*.

Kowta, M. (1963). *Old Togiak in prehistory.* University of California, Los Angeles.

Lader, R., J. E. Walsh, U. S. Bhatt, and P. A. Bieniek (2020). Anticipated changes to the snow season in Alaska: Elevation dependency, timing and extremes. *International Journal of Climatology 40*, 169–187.

Lebreton, J., J. D. Nichols, R. J. Barker, R. Pradel, and J. A. Spendelow (2009). Modeling individual animal histories with multistate capture–recapture models. *Advances in Ecological Research 41*, 87–173.

Macander, M. J., P. R. Nelson, T. Nawrocki, G. V. Frost, K. Orndahl, E. C. Palm, A. F. Wells, and S. J. Goetz (2022). Time-series maps reveal widespread change in plant functional type cover across arctic and boreal Alaska and Yukon. *Environmental Research Letters 17*(5), 054042.

Oates, B. A., K. L. Monteith, J. R. Goheen, J. A. Merkle, G. L. Fralick, and M. J. Kauffman (2021). Detecting resource limitation in a large herbivore population is enhanced with measures of nutritional condition. *Frontiers in Ecology and Evolution 8*.

Quéroué, M., C. Barbraud, F. Barraquand, D. Turek, K. Delord, N. Pacoureau, and O. Gimenez (2021). Multispecies integrated population model reveals bottom-up dynamics in a seabird predator–prey system. *Ecological Monographs 91*(3), e01459.

Ruprecht, J. S., D. N. Koons, K. R. Hersey, N. T. Hobbs, and D. R. MacNulty (2020). The effect of climate on population growth in a cold-adapted ungulate at its equatorial range limit. *Ecosphere 11*, e03058.

Schaub, M., O. Gimenez, A. Sierro, and R. Arlettaz (2007). Use of integrated modeling to enhance estimates of population dynamics obtained from limited data. *Conservation Biology 21*(4), 945–955.

Schaub, M. and M. Kery (2021). *Integrated population models: theory and ecological applications with R and JAGS*. Academic Press.

Schmidt, J. H., M. D. Cameron, K. Joly, J. M. Pruszenski, J. H. Reynolds, and M. S. Sorum (2022). Bayesian spatial modeling of moose count data: increasing estimator efficiency and exploring ecological hypotheses. *The Journal of Wildlife Management*, e22220.

Sexton, J. P., P. J. McIntyre, A. L. Angert, and K. J. Rice (2009). Evolution and ecology of species range limits. *Annual Review of Ecology, Evolution and Systematics 40*(1), 415–436.

Skoog, R. O. (1968). *Ecology of the caribou (Rangifer tarandus granti) in Alaska.* University of California, Berkeley.

Szűcs, M., M. Vahsen, B. Melbourne, C. Hoover, C. Weiss-Lehman, and R. Hufbauer (2017). Rapid adaptive evolution in novel environments acts as an architect of population range expansion. *Proceedings of the National Academy of Sciences 114*(51), 13501–13506.

Tape, K. D., D. D. Gustine, R. W. Ruess, L. G. Adams, and J. A. Clark (2016). Range expansion of moose in arctic Alaska linked to warming and increased shrub habitat. *PLoS ONE 11.*

Valkenburg, P., R. A. Sellers, R. C. Squibb, J. D. Woolington, A. R. Aderman, and B. W. Dale (2003). Population dynamics of caribou herds in southwestern Alaska. *Rangifer 23*(5), 131–142.

Walsh, J. E. and B. Brettschneider (2019). Attribution of recent warming in Alaska. *Polar Science 21*, 101–109.

Appendix

5.1 Chapter 2: Supplementary Tables & Figures

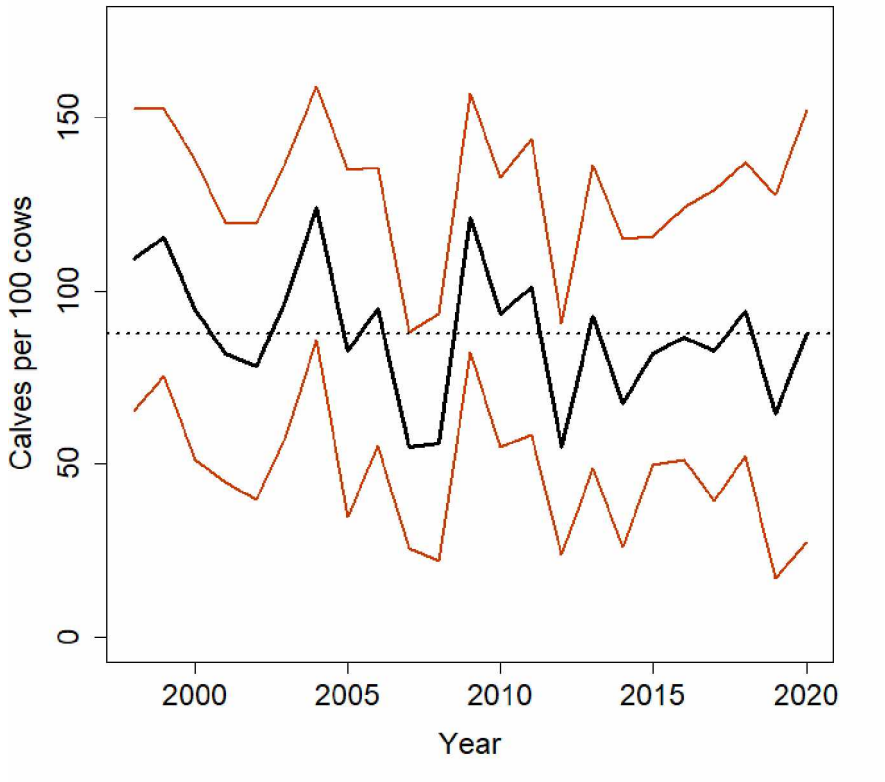

Figure 5.1: Annual calves per 100 cows produced in the spring, a derived quantity from the multistate model calculated using annual parturition and twinning posterior distributions. Red lines indicate 95% credible intervals.

Table 5.1: State and observation matrices for the capture event

(a) The matrix $\mathbf{\Omega}$ representing the state process for the capture event

$y_{i,t}$			
no calf	one calf	twins	dead
ϕ_{cw}	$\phi_{cw}(\phi_{ca})$	$\phi_{cw}(\phi_{ca})^2$	0

(b) The matrix $\mathbf{\Theta}$ representing the observation process for the capture event

		$y_{i,t}$			
		no calf	one calf	twins	dead
$z_{i,t}$	no calf	1	0	0	1
	one calf	0	1	0	1
	twins	0	0	1	1
	dead	0	0	0	1

Table 5.2: State and observational matrices for moose in Togiak National Wildlife Refuge for the multistate model. ϕ_{cw} represents cow survival probability, ϕ_{ca} represents calf survival probability, α represents parturition probability, γ represents twinning probability (given a cow has given birth), and p_{ca} represents calf detection probability.

(a) The state process for the first month

$t \in$ Month 1		$z_{j,t+1}$			
		no calf	one calf	twins	dead
$z_{j,t}$	no calf	$\phi_{cw}(1-\alpha)$	$\phi_{cw}\alpha(1-\gamma)$	$\phi_{cw}\alpha\gamma$	$(1-\phi_{cw})$
	one calf	$\phi_{cw}(1-\alpha)(\phi_{ca}(1-\phi_{ca}))$	$\phi_{cw}\alpha(1-\gamma)(\phi_{ca}(1-\phi_{ca}))$	$\phi_{cw}\alpha\gamma(\phi_{ca}(1-\phi_{ca}))$	$(1-\phi_{cw})$
	twins	$\phi_{cw}(1-\alpha)(\phi_{ca}(1-\phi_{ca}))^2$	$\phi_{cw}\alpha(1-\gamma)(\phi_{ca}(1-\phi_{ca}))^2$	$\phi_{cw}\alpha\gamma(\phi_{ca}(1-\phi_{ca}))^2$	$(1-\phi_{cw})$
	dead	0	0	0	1

(b) The state process for all months

$t \notin$ Month 1		$z_{j,t+1}$			
		no calf	one calf	twins	dead
$z_{j,t}$	no calf	ϕ_{cw}	0	0	$(1-\phi_{cw})$
	one calf	$\phi_{cw}(1-\phi_{ca})$	$\phi_{cw}\phi_{ca}$	0	$(1-\phi_{cw})$
	twins	$\phi_{cw}(1-\phi_{ca})^2$	$\phi_{cw}\phi_{ca}(1-\phi_{ca})$	$\phi_{cw}\phi_{ca}^2$	$(1-\phi_{cw})$
	dead	0	0	0	1

(c) The observation process for all observations following initial collaring event.

		$y_{j,t}$			
		no calf	one calf	twins	dead
$z_{j,t}$	no calf	1	0	0	0
	one calf	$1-p_{ca}$	p_{ca}	0	0
	twins	$(1-p_{ca})^2$	$1-p_{ca}$	p_{ca}	0
	dead	0	0	0	1

Table 5.3: Posterior distributions of random effect standard deviations for demographic parameters. All means were set to zero. Year and individual as random effects were included in all four logistic regressions to account for inter-year and inter-individual variation and obtain annual and individual estimates. GMU as a random effect was included in the cow survival regression to account for suspected spatial variability due to differing hunting management. 2.5% and 97.5% BCI refer to lower and upper 95% Bayesian Credible Intervals. All $\hat{R}$ values were at or below 1.1 and indicated sufficient convergence for all coefficients.

regression	random effect	mean σ	2.5% BCI	97.5% BCI
p(cow survival)	Year	0.47	0.03	1.00
p(calf survival)	Year	3.51	2.12	5.79
p(parturition)	Year	0.73	0.33	1.26
p(twinning)	Year	0.91	0.06	2.26
p(cow survival)	GMU	1.38	0.09	4.71
p(cow survival)	Individual	0.27	0.01	0.78
p(calf survival)	Individual	2.67	1.84	3.81
p(parturition)	Individual	0.67	0.17	1.19
p(twinning)	Individual	0.75	0.03	2.06

Table 5.4: Summary of simple linear regressions between time, environmental covariates, and the Pacific Decadal Oscillation (PDO). KS refers to the long-term weather station in King Salmon, Alaska, USA, where we aggregated data from daily observations to either July (summer) or Nov-April (winter).

Regression	Time Period	Slope	Std. Err	p-value
NDVI $\sim$ Time	2000-2020	1.96	1.25	0.13
NDVI $\sim$ PDO	2000-2020	0.82	0.25	$<$0.005
WSI $\sim$ Time	2001-2019	-0.18	1.33	0.90
WSI $\sim$ PDO	2001-2019	-0.48	0.13	$<$0.005
KS Summer $\sim$ Time	1970-2020	0.03	0.01	$<$0.05
KS Winter $\sim$ Time	1970-2020	0.06	0.02	$<$0.05
NDVI $\sim$ KS Summer	2000-2020	0.58	0.11	$<$0.0005
WSI $\sim$ KS Winter	2001-2019	-0.26	0.07	$<$0.005

Table 5.5: Summary of covariate coefficient posterior distributions from the four logistic regressions performed within the multistate model. 2.5% and 97.5% BCI refer to lower and upper 95% Bayesian Credible Intervals, and f refers to the proportion of the posterior distribution with the same sign as the mean. All $\hat{R}$ values were at or below 1.1, indicating sufficient convergence for all coefficients.

regression	covariate	mean	sd	2.5% BCI	97.5% BCI	f
p(cow survival)	β_{ndvi}	0.12	0.18	-0.24	0.46	0.76
p(calf survival)	β_{ndvi}	1.31	0.78	-0.27	2.80	0.95
p(parturition)	$\beta_{ndvi_{t-1}}$	0.06	0.22	-0.37	0.49	0.62
p(twinning)	$\beta_{ndvi_{t-1}}$	0.53	0.38	-0.16	1.35	0.94
p(cow survival)	β_{wsi}	0.01	0.17	-0.33	0.35	0.53
p(calf survival)	β_{wsi}	-0.58	0.74	-2.09	0.89	0.79
p(parturition)	$\beta_{wsi_{t-1}}$	0.05	0.20	-0.36	0.45	0.62
p(twinning)	$\beta_{wsi_{t-1}}$	-0.59	0.46	-1.63	0.18	0.93
p(cow survival)	β_{age}	-0.67	0.17	-1.02	-0.36	1.00
p(calf survival)	β_{age}	-0.31	0.36	-1.02	0.40	0.81
p(parturition)	β_{age}	-0.83	0.19	-1.24	-0.48	1.00
p(twinning)	β_{age}	1.47	0.75	0.24	3.13	1.00
p(cow survival)	β_{age^2}	-0.02	0.12	-0.24	0.23	0.57
p(calf survival)	β_{age^2}	-0.14	0.25	-0.65	0.34	0.73
p(parturition)	β_{age^2}	-0.23	0.19	-0.62	0.13	0.88
p(twinning)	β_{age^2}	0.13	0.56	-0.88	1.31	0.57

Table 5.6: Pearson's correlation coefficients for correlations of means between demographic parameters. ρ values < 0.6 indicate that random effects are independent from one another across individuals.

Correlation	Pearson's ρ
s(cow)∼s(calf)	0.02
s(cow)∼p(parturition)	-0.06
s(cow)∼p(twinning)	0.03
s(calf)∼p(parturition)	0.17
s(calf)∼p(twinning)	-0.03
p(parturition) ˜ p(twinning)	0.03

5.2 Chapter 3: Supplementary Tables & Figures

Table 5.7: Parturition rates for various moose populations across North America. We used these rates to create a representative Beta distribution, which we then used as an informative prior for annual parturition estimates in the IPM.

state	time period	study duration (yr)	rate	source
AK	1994-1996	2	0.80	Testa (2002)
AK	1998-2000	2	0.89	Bertram and Vivion (2002)
WY	2011-2014	3	0.75	Oates et al. (2021)
WA	2014-2018	4	0.70	Harris et al. (2021)
AK	1976-1986	10	0.81	Ballard et al. (1991)
AK	2002-2012	10	0.78	Boertje et al. (2019)
AK	1994-2005	11	0.82	Boertje et al. (2007)
AK	1994-2005	11	0.86	Boertje et al. (2007)
AK	1994-2005	11	0.87	Boertje et al. (2007)
AK	1994-2005	11	0.90	Boertje et al. (2007)
AK	1998-2013	15	0.77	Aderman (2014)

5.3 References

Aderman, A. (2014). Monitoring moose demographics at Togiak National Wildlife Refuge, southwestern Alaska, 1998-2013. *Togiak National Wildlife Refuge, Dillingham, Alaska.*, 1–25.

Ballard, W. B., J. S. Whitman, and D. J. Reed (1991). Population dynamics of moose in south-central Alaska. *Wildlife Monographs*, 3–49.

Bertram, M. R. and M. T. Vivion (2002). Moose mortality in eastern interior Alaska. *The Journal of Wildlife Management 66*, 747–756.

Boertje, R. D., G. G. Frye, and D. D. Young (2019). Lifetime, known-age moose reproduction in a nutritionally stressed population. *Journal of Wildlife Management 83*, 610–626.

Boertje, R. D., K. A. Kellie, C. T. Seaton, M. A. Keech, D. D. Young, B. W. Dale, L. G. Adams, and A. R. Aderman (2007). Ranking Alaska moose nutrition: Signals to begin liberal antlerless harvests. *Journal of Wildlife Management 71*, 1494–1506.

Harris, R. B., J. Goerz, J. Oyster, R. C. Cook, K. Mansfield, M. Atamian, C. Lowe, A. Prince, and B. Y. Turnock (2021). Bottom-up and top-down factors contribute to reversing a moose population increase in northeastern Washington. *Alces 57*, 47–69.

Oates, B. A., K. L. Monteith, J. R. Goheen, J. A. Merkle, G. L. Fralick, and M. J. Kauffman (2021). Detecting resource limitation in a large herbivore population is enhanced with measures of nutritional condition. *Frontiers in Ecology and Evolution 8*.

Testa, J. W. (2002). Does predation on neonates inherently select for earlier births? *Journal of Mammalogy 83*, 699–706.